RELIABILITY- BASED OPTIMUM INSPECTION PLANNING FOR COMPONENTS SUBJECTED TO FATIGUE INDUCED DAMAGE

A Thesis

by

JASMINE GULATI

Submitted to the Office of Graduate and Professional Studies of
Texas A&M University
in partial fulfillment of the requirements for the degree of

MASTER OF SCIENCE

Chair of Committee,	Arash Noshadravan
Committee Members,	Petros Sideris
	Homero Castaneda-Lopez
Head of Department,	Robin Autenrieth

August 2018

Major Subject: Civil Engineering

ABSTRACT

The degradation of metallic systems under cyclic loading is prone to significant uncertainty. This uncertainty in turn affects the reliability in the prediction of residual lifetime and the subsequent decision regarding the optimum inspection and maintenance schedules. In particular, the experimental data on the evolution of fatigue-induced cracks shows significant scatter stemming from initial flaws, metallurgical heterogeneities, and randomness in material properties like yield stress and fracture toughness. The objective of this research is to improve the reliability-based optimal inspection planning of metallic systems subjected to fatigue, taking into account the associated uncertainty. To that end, this research aims to address the two main challenges faced in developing a credible reliability-based framework for lifecycle management of fatigue-critical components. The first challenge is to construct a stochastic model that can adequately capture the nonlinearity and uncertainty observed in the crack growth histories. The second one involves presenting a computationally efficient strategy for solving the stochastic optimization associated with optimum maintenance scheduling. In order to fulfill these objectives, a Polynomial Chaos (PC) representation is constructed of fatigue-induced crack growth process using a database from a constant amplitude loading experiment. The PC representation relies on expanding the crack growth stochastic process on a set of random basis functions whose coefficients are estimated from the experimental database. The probabilistic model obtained is then integrated into a reliability framework that

minimizes the total expected life-cycle cost of the system subjected to constraints in terms of time to inspections, and the maximum probability of failure defined by the limit state function. Lastly, an efficient and accurate optimization strategy that uses surrogate models is suggested to solve the stochastic optimization problem. The sensitivity of the optimum solution to the level of risk is also examined. This research aims to provide a decision support tool for informed decision-making under uncertainty in the life-cycle planning of systems subjected to fatigue failure.

DEDICATION

To my parents, my sister and my brother.

ACKNOWLEDGEMENTS

First and foremost, I would like to express my deepest gratitude to my research advisor, Dr. Arash Noshadravan, for his constant support, his endless patience and his invaluable suggestions on every aspect of this work. This thesis has been anything but easy, and it would not have been possible without his guidance. I would also like to thank my committee members, Dr. Petros Sideris and Dr. Homero Castaneda-Lopez, for their comments and suggestions for improvement of this work.

I would like to thank my friend, Tobia Rinaldo, for his suggestions and insight, especially at times when I needed it the most. Furthermore, I would like to thank my friend, Rajat Kothari, for always believing in me and supporting me.

I am sincerely thankful to my friends and colleagues, as well as the department faculty and staff for making my time at Texas A&M University a memorable one.

Finally, a huge thank you to my parents and siblings who have always pushed me to seek boundaries I thought were impossible for me.

CONTRIBUTORS AND FUNDING SOURCES

Contributors

This work was supported by a thesis committee consisting of Dr. Arash Noshadravan and Dr. Petros Sideris of the Department of Civil Engineering and Dr. Homero Castaneda-Lopez of the Department of Materials Science and Engineering.

All other work conducted for the thesis was completed by the student independently.

Funding Sources

There are no outside funding contributions to acknowledge related to the research and compilation of this document.

NOMENCLATURE

CGR	Crack Growth Rate
GP	Gaussian Process
LEFM	Linear Elastic Fracture Mechanics
MSE	Mean Squared Error
PC	Polynomial Chaos
PDF	Probability Density Function
SIF	Stress Intensity Factor
SRCC	Spearman's Rank Correlation Coefficient

TABLE OF CONTENTS

Page

LIST OF FIGURES

Page

LIST OF TABLES

Page

1. INTRODUCTION

1.1. Overview

Structures as a whole or their individual components degrade over time making them susceptible to partial or complete failure. Several phenomenon like corrosion, fatigue, creep and ageing may contribute to this time-dependent deterioration of structures. In order to ensure that the structure remains safe and operable during its complete service life, it is imperative to schedule inspection and maintenance actions. To this end, the lifecycle management of structures can be defined in terms of two models: a degradation model and a decision model [1](Figure1).

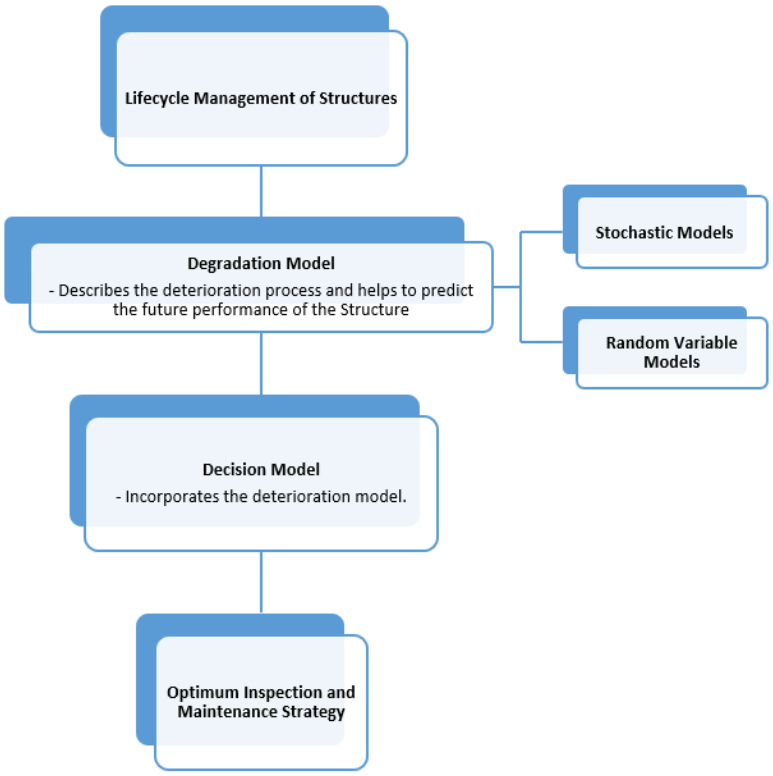

Figure 1: Integrity Management of Structures

The degradation model is used to describe the exact deterioration phenomenon under consideration and helps in predicting the future performance of the structure. There is no way in which the exact state of the structure in future can be known, thus these models depict the performance in a probabilistic way. This could be either achieved by defining the process by a stochastic model or by replacing parameters of deterministic models by random variables. A decision model then incorporates this deterioration model to arrive at an optimum inspection and maintenance schedule.

Maintenance actions are scheduled several times during the design life of the structure. These actions can be broadly classified into two types: preventive actions and performance-based or condition-based actions. The intent of preventive maintenance actions is to delay the deterioration process and are generally carried out at predefined intervals during the lifetime of the structure. On the other hand, performance- based maintenance actions are carried out when there is a likelihood of the performance criteria of the structure to be violated. These maintenance actions improve the state of the system by either bringing it back to its original condition or to a state closer to its original condition. Several recent studies are focused on the optimization of these performance-based maintenance activities [2] [3] [4] [5] [6] [7] [8]. The decision model facilitates in carrying out this optimization. A well-known way of defining the optimum schedule is defining it in terms of the lifecycle costs wherein, the decisions regarding maintenance activities are made taking into account not only the safety of the structure but also the costs.

Fatigue- induced cracks are a major cause for the deterioration of metallic components subjected to cyclic loading. The crack grows with each applied load cycle leading to a reduction in the components structural performance. This research addresses the deterioration in metallic components due to fatigue and furthermore, aims to provide a decision support tool for making credible decisions regarding their lifecycle management. The crack growth process shows significant scatter due to the randomness in material properties such as fracture toughness and yield stress, metallurgical inhomogeneity, stresses applied and initial crack sizes. In this research, a stochastic model is developed that takes into account all these uncertainties and subsequently, integrates it into a reliability framework to work out an optimum inspection and repair schedule for the component. An optimal inspection schedule herein corresponds to a schedule with minimum total expected lifecycle costs while guaranteeing that the probability of failure throughout the lifetime does not exceed a threshold value.

Optimal planning of maintenance schedules for structures under fatigue has been addressed in several previous works. Gomes et al. [9] obtained an optimal maintenance schedule for a rectangular plate having a center-cracked tension geometry. The optimum maintenance schedule was defined in terms of three design variables: the crack repair size, the time to first inspection and the time intervals between the following inspections. The optimization problem involved a discontinuous objective function and was solved using a multi-start simplex approach. Beaurepaire et al. [10] used reliability- based optimization techniques to arrive at an optimum schedule. The authors developed an optimum maintenance schedule for a plate with two rivet holes in terms two design variables: the

time to the one and only inspection activity considered and the quality of inspection method. The crack initiation and the crack propagation phenomenon were modelled using cohesive zone elements. The optimization problem was solved used a gradient-based technique. Valdenbenito and Schueller [11] similarly solved the problem of inspection planning in context of a reliability-based framework. The optimum maintenance schedule again was defined in terms of two design variables: the quality of inspection method and the time to the one and only inspection activity considered. Paris- Erdogan law [12] was used to model the crack growth phenomenon and the authors solved the optimization problem using a gradient-based approach. It was concluded that the optimal solution is a compromise between the costs of different actions: inspections, repairs and failures. If the happening of these events is minimized individually, then the solution achieved would not be optimum.

Despite the recent advancements made in the field of lifecycle management of fatigue-critical components, challenges still exist that prevent making more informed decisions regarding the same. The credibility of the decisions taken depends on the degradation and decision models employed and the efficiency of the optimization strategy. The fatigue crack growth process shows significant scatter and very few models exist in literature that can capture the fatigue crack growth phenomena accurately. Additionally, the reliability-based framework adopted to obtain the optimal inspection plan for components under fatigue can be improvised by taking into account different scenarios like multiple inspection activities or multiple repair efforts.

The above two challenges are well tackled in this research. The stochastic model developed herein is constructed directly from field observations and can capture the actual random process accurately. The decision model adopted allows for multiple inspection events and different repair efforts depending upon the condition of the system, thereby ensuring the model represents the actual repair effort taken in the field. Lastly, an efficient optimization strategy using Gaussian process regression model is presented to solve the stochastic optimization problem associated with the optimal maintenance planning of components under fatigue.

This study has been organized in the following way. In the subsequent section, the methodology used for modelling the fatigue crack growth process using a polynomial chaos formalism has been described. The reliability- based framework and formulation of the stochastic optimization problem has been highlighted in section 3. Section 3 also presents an efficient strategy for solving the optimization problem. Finally, in section 4 the proposed methodology has been implemented on a structural component to develop its optimal maintenance schedule.

1.2. Research Objective

This research aims to provide a reliability- based decision support tool for making informed decisions regarding the lifecycle planning of systems subjected to fatigue-induced damage while taking into account the associated uncertainties. The proposed decision shall be the optimum solution for the inspection and maintenance schedule to be adopted that minimizes the total expected life-cycle costs of the system while ensuring that the probability of failure is always above a given threshold. The total expected life-

cycle costs include the initial cost, the costs of inspections, the cost of repairs and the cost of failures.

The three specific objectives of this research can be summarized as follows:

1. Construction of a stochastic model that can adequately capture the non-linearity and uncertainty observed in the crack growth phenomenon.
2. Present a reliability- based formulation for optimum maintenance scheduling that minimizes the total expected lifecycle cost.
3. Present a computationally efficient strategy for solving the stochastic optimization associated with the optimum scheduling.

2. DETERIORATION MODELING FOR FATIGUE

2.1. Background

Cracks may develop and grow under repeated cyclic loading on structures. The presence of these cracks reduces the structural performance and may result in the failure of the structure below its maximum strength. Two main approaches have been adopted to predict the fatigue life of structures: S-N Approach and the Linear Elastic Fracture Mechanics (LEFM) approach. The S-N curves have been one of the oldest used approaches to determine the fatigue life of structures. These curves relate the total fatigue life of the structure to constant stress amplitudes. The total fatigue life of the structure accounts for the cycles spent in both the crack initiation period and the crack propagation period. However, this approach does not give an explicit relation between the crack length and the number of loading cycles and hence, cannot be suitably integrated into a reliability framework.

2.1.1. Linear Elastic Fracture Mechanics (LEFM)

The basic principle underlying the fracture mechanics approach is that the stresses ahead of the crack tip in any structural element can be explained completely by a single parameter known as stress intensity factor (SIF) K. The value of this parameter is dependent on the crack size and the magnitude of the stresses applied on the element. The growth of crack under repeated cyclic loading is termed as fatigue. There are three stages that define the fatigue crack propagation process: the crack initiation stage, the stable crack growth stage and the unstable crack growth stage. The time taken by micro-cracks to

nucleate to form larger cracks that may grow corresponds to the time spent in the crack initiation stage. It is represented by Region I in Figure 2. This region is characterized by a threshold value of stress intensity factor range ΔK_{th} . If the SIF range ΔK is below this value, then the crack will not propagate. The crack initiation period varies according to the element being studied [11]. For welds, this period is almost negligible and can be ignored [11]. On the other hand, for aerospace elements that follow higher standards of manufacturing and assembling this stage may account for the entire lifetime [11].

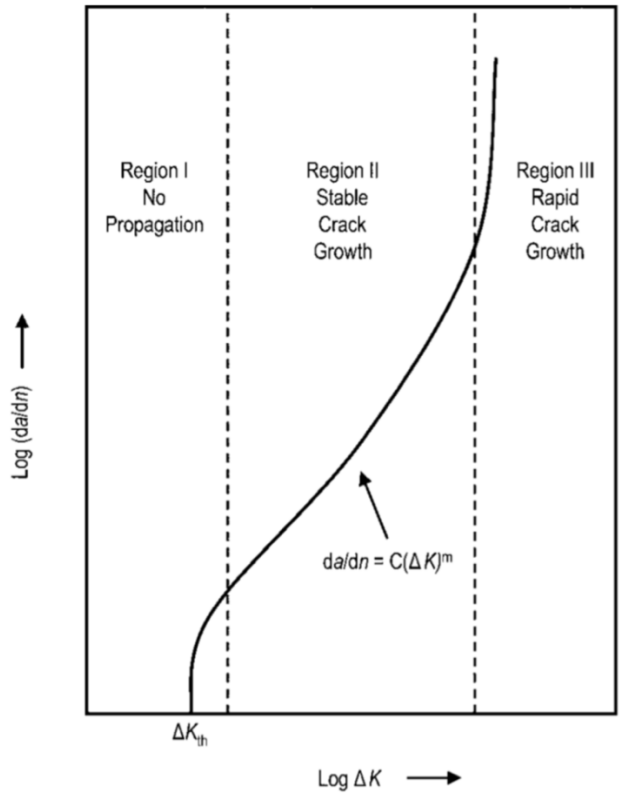

Figure 2: Crack Growth Rate versus Stress Intensity Factor Range [13]

Stable crack growth is represented by Region II in Figure 2. In this stage, the crack propagates with each applied load cycle and if its propagation is not limited, then it may

lead to the failure of the structure. The crack growth rate (CGR) follows a linear relationship with the SIF range on a log-log scale in this region. This relationship is described by Paris Law. LEFM accounts for the time spent by the crack in the crack propagation stage or the stable crack growth stage. Region III in Figure 2 accounts for the unstable crack growth stage where the crack advances at a very fast rate leading to fracture. This stage is ignored for design purposes.

Fracture can be defined as a tension failure mode in which the component breaks into two parts losing its load carrying capacity in entirety leading to failure of the structure. Fracture failures in structures could be either ductile, brittle or a combination of both. Ductile fracture is associated with plastic yielding before failure, thus it is the preferred mode of failure as it gives sufficient warning. Brittle fracture on the other hand gives little or no warning at all. In this case the structure fails before reaching its ultimate capacity. This is tantamount to the unstable crack growth stage. In this failure mode, the SIF attains a critical value known as the fracture toughness, which is a material property and is a measure of the ability of the material to resist brittle fracture.

2.2. Fatigue Models in Literature

As mentioned previously, deterioration models predict the future performance of the structure in a probabilistic fashion. There are mainly two types of models that can be used for degradation modeling: Random variable models and Stochastic Models.

2.2.1. Random Variable Models

In these models, random variables are substituted in place of the deterministic parameters in continuum crack propagation laws. These random variables then account for the

uncertainty associated with the process. Most of these models are based on Paris Law [12] which can be represented by the following equation:

$$\frac{da}{dN} = C(\Delta K)^m \tag{2.1}$$

where, C and m are material parameters and assume probabilistic distributions in this case.

This is a very common approach; however, it has some drawbacks. The major disadvantage of using this method is that most of these models are based on a randomized version of Paris Law while it has been mentioned in literature [14] that other laws like Forman's Law can describe the process better.

2.2.2. Stochastic Models

Several stochastic models have been reported in literature for the modeling of fatigue crack growth phenomenon [15]. Yang and Manning [16] extend the concept of lognormal random variable model to represent the crack growth rate. Kozin and Bogdanoff [17] and Ghonem and Provan [18] have used a discontinuous markov process to represent the crack growth phenomenon. The concepts developed in [18] have been extended by Ghonem and Dore [14] to describe the scatter associated with crack growth process at any stress level in terms of constant probability curves. Guida and Penta [19] propose a stochastic model in which the time to reach a specified crack length is modeled by a gamma process. The shape parameter for the gamma distribution is assumed to depend on the crack length. Ortiz and Kiremidjian [20] [21]in their probabilistic model assume that the CGR is comprised of two components: a low frequency component and a high frequency

component. The low frequency component is representative of the mean behavior and they use a randomized version of Paris law to describe this part. The distributions of the parameters of the crack growth law are determined from an experimental dataset. The high cycle frequency component, which is responsible for the scatter observed in the process, is modeled as random noise and is completely characterized by its auto covariance function.

In this research, the crack growth process is described by a stochastic model that is based on polynomial chaos expansions constructed from experimental data.

2.3. A Polynomial Chaos Approach for Modelling Fatigue Growth

2.3.1. Overview of the Polynomial Chaos Method

Polynomial Chaos (PC) expansions serve as an efficient tool for describing dynamic systems [22] and for propagating the associated uncertainties into the model predictions. A second order random variable X having finite variance can be expressed by the following expansion:

$$X(\xi) = \sum_{i=0}^{\infty} c_i \psi_i(\xi) \tag{2.2}$$

Herein, c_i are known as the polynomial chaos coefficients which are deterministic in nature and $\psi_i(.)$ are polynomials involving all combinations of the n random variables $\{\xi\}_{j=1}^{n}$ [23] . The parameter n refers to the stochastic dimension of the polynomial. These polynomials fulfill orthogonality conditions with respect to a given probability density measure which is a characteristic of the underlying random variable ξ_j . The orthogonality condition can be expressed as follows:

$$\mathrm{E}\left[\psi_m\left(\xi_j\right)\psi_m\left(\xi_j\right)\right]=1 \tag{2.3}$$

The expansion represented by Eq. (2.2) needs to be trimmed to a fixed number of terms P which is can be computed by the following equation:

$$P+1=\frac{(n+m)!}{n!m!} \tag{2.4}$$

where, m represents the order of the polynomial. The accuracy of the expansion thus relies on the order of the polynomials selected and also on the choice of the underlying random variables [24]. The expansion can then be modified and represented as follows:

$$X\left(\xi\right)=\sum_{i=0}^{P}c_i\psi_i\left(\xi\right) \tag{2.5}$$

The choice of the PC basis is governed by the choice of the underlying random variables [24]. Hermite family of orthogonal polynomials are used if underlying random variables are Gaussian. Similarly, Legendre polynomials are used when uniform random variables are chosen and Laguerre polynomials are chosen if the underlying random variables follow gamma distributions. In this research, the underlying random variables are assumed to be uniformly distributed and thus the corresponding chosen PC basis are Legendre polynomials. The polynomials can be given by:

$$\psi_0(\xi_i)=1 \tag{2.6}$$

$$\psi_1(\xi_i)=\xi_i \tag{2.7}$$

$$\psi_{n+1}(\xi_i)=\frac{2n+1}{n+1}\xi_i\psi_n(\xi_i)-\frac{n}{n+1}\psi_{n-1}(\xi_i),\quad n\geq 2 \tag{2.8}$$

The PC coefficients are calculated by making use of the orthogonal nature of the PC basis. The expression used to evaluate PC coefficients is given by:

$$c_i = \frac{\mathrm{E}[X(\xi)\psi_i(\xi)]}{\mathrm{E}[\psi_i^2(\xi)]} \tag{2.9}$$

The denominator in Eq. (2.9) can be readily determined for any orthogonal family of polynomials. In case of Legendre polynomials, the value of this denominator can be given by:

$$\mathrm{E}[\psi_i^2(\xi)] = \frac{1}{2i+1} \tag{2.10}$$

The calculation of the numerator requires the following integral formulation to be solved:

$$\mathrm{E}[X(\xi)\psi_i(\xi)] = \int_{S_\xi} X(\xi)\psi_i(\xi)p_\xi(\xi)d\xi \tag{2.11}$$

where, S_ξ is the support of ξ and p_ξ is the marginal probability density function of ξ. The evaluation of this numerator requires the mapping $\xi \to X(\xi)$ be established. Before elaborating further on the methodology used for the determination Eq.(2.11), it should be noted that the expansion given by Eq. (2.5) can be readily extended to represent second-order random processes in which the coefficients are now representative of the physical dimension of the process. A stochastic process X that is represented over a finite subset of physical dimension t can be then expressed as:

$$X(t,\xi) = \sum_{i=0}^{P} c_i(t)\psi_i(\xi) \tag{2.12}$$

2.3.2. Construction of PC expansions representing random processes using experimental data

The methodology adopted in this research for constructing the PC expansion representing the stochastic process is based on the work of Das et al [25]. The actual random deterioration process is modeled as a stochastic process given by $X(t,\xi)$. The process can be discretized over an n -finite subset of its physical dimension t. The process now consists of n components and be given by:

$$X = [x_1, x_2, ...x_n]^T \tag{2.13}$$

Where, T is the transpose operator.

Each of these n random variable components can be represented by a PC expansion given by:

$$x_j \equiv x_j(\xi_j) = \sum_{i=0}^{P} c_{j,i}\psi_i(\xi_j) \tag{2.14}$$

This formulation is similar to the one shown in Eq. (2.5). Similarly, now Eq. (2.9) used for determination of Chaos coefficients can be rewritten as:

$$c_{j,i} = \frac{\mathrm{E}[x_j(\xi_j)\psi_i(\xi_j)]}{\mathrm{E}[\psi_i^2(\xi_j)]} \tag{2.15}$$

As mentioned previously, the computation of the numerator of the above equation requires the mapping $\xi_j \to x_j(\xi_j)$ which is constructed using Rosenblatt transformation. According to Rosenblatt transformation [26], the left-hand side and right-hand side of the equation given below are equal in distribution sense.

$$P_{\xi_j}(\xi_j) = P_j(x_j) \tag{2.16}$$

where, $P_{\xi_j}(\xi_j)$ and $P_j(x_j)$ are two random variables, both of which have their PDF as uniform distributions supported on $[0,1]$. Thus, Eq. (2.16) can be rewritten as:

$$x_j = P_j^{-1} P_{\xi_j}(\xi_j) \tag{2.17}$$

Now, rewriting Eq. (2.14) incorporating Eq. (2.17):

$$x_j = P_j^{-1} P_{\xi_j}(\xi_j) = \sum_{i=0}^{P} c_{j,i} \psi_i(\xi_j) \tag{2.18}$$

Thus, Eq. (2.15) can now be written as:

$$c_{j,i} = \frac{\mathrm{E}[P_j^{-1} P_{\xi_j}(\xi_j)\psi_i(\xi_j)]}{\mathrm{E}[\psi_i^2(\xi_j)]} \tag{2.19}$$

The solution to $P_j^{-1} P_{\xi_j}$ require solving an integral equation for each ξ_j that has a high computational burden. In order to avoid this, the following has been solved using a surrogate function. It is essential to note that in this approach, the marginal PDF of x_j are used to define the mapping, thus making it more appropriate to represent P_j^{-1} as $P_{x_j}^{-1}$. This marginal distribution for each x_j is obtained by linearly interpolating the normalized marginal histogram at the particular x_j .

The dependency between the different components of $(x_j)_{j=1}^n$ is characterized by the dependency between the random variables $(\xi_j)_{j=1}^n$. Initially, the Spearman's rank correlation coefficient matrix (SRCC) between the different components is found out using the experimental data. The size of this matrix ρ_s is nXn. The SRCC matrix does not change under monotonic transformation and this property of it has been utilized to characterize the dependencies between the random variables. The samples of the random variables are generated such that they have the same SRCC matrix as the experimental data and then, the samples of the random variables obtained for each component are put

back into the PC expansion obtained for the respective component. This ensures that the realizations generated to depict the random process will be consistent with the original stochastic process.

The construction of the model is thus solely done by using the information known about the marginal PDF of the components and the SRCC matrix. Once the model has been constructed, it is synthetically used to generate realizations of the process that capture the evolution of damage in the structure. This information is then integrated into a reliability-based lifecycle management framework.

3. DECISION MODELING

As discussed previously, structures need to be inspected and repaired in time such that a check can be maintained on their time- dependent degradation, thereby ensuring they remain safe for operation throughout their lifetime. The stochastic model developed herein adequately captures the randomness in the crack growth histories and appropriately propagates it into the limit state functions and the reliability framework. This section discusses the reliability-based framework adopted in this study.

3.1. Limit State Functions

State functions are generally representative of the difference between the maximum load the structure can withstand and the actual load applied. It can take a value greater than zero as long as the former is higher than the latter. Since structures deteriorate over time the positive value of these functions decreases over time. This instant at which this function attains a value of zero is known as the limit state and this point in time corresponds to failure in the structure. These functions play a very integral part in reliability assessment of structures and are responsible for characterizing the failure mode. These in turn can also assist in deciding the kind of maintenance action which should be taken once an inspection activity is carried out.

In context of LEFM, the instant at which SIF K_I exceeds the fracture toughness K_{IC} of the material, a failure event is considered to occur. This type of failure can be termed as brittle failure. However, the failure of a component may also occur when the maximum capacity of the component is exceeded (ductile failure) or may occur due to the collective

effect of the above two reasons. The R6 curve [27] takes into account all the above cases and thus, is an appropriate way to define the failure event. The limit state function for the failure event can be given by:

$$G_f(a(t)) = K_{IC}C_f(a(t)) - K_I(a(t)) \tag{3.1}$$

Where, K_{IC} is representative of the fracture toughness of the material and varies with the type of material, $K_I(a(t))$ is the value of the SIF at a particular crack length, $a(t)$ which in turn is a function of time t, and $C_f(a(t))$ is a factor given by the following equation:

$$C_f(a(t)) = \frac{\sigma_{\max}}{\sigma_c(a(t))}\left(\frac{8}{\pi^2}\log\left(\sec\left(\frac{\pi\sigma_{\max}}{2\sigma_c(a(t))}\right)\right)\right)^{-1/2} \tag{3.2}$$

Where, $\sigma_{\max}$ is the maximum stress applied and $\sigma_c(a(t))$ is known as the collapse stress. It is dependent on the crack length, however for a component under axial tension it is taken equal to the yield stress σ_y. The value of the SIF at any crack length $a(t)$ can be evaluated using the following equation:

$$K_I(a(t)) = Y(a(t))\sqrt{\pi a(t)}\sigma_{\max} \tag{3.3}$$

where, $Y(a(t))$ is a geometry function.

The decrease in the value of the limit state function can be attributed to the crack length growing in time. The limit state function also includes several other parameters in its formulation that have uncertainty associated with them. There is randomness in the initial crack size which is accounted for by modeling it as a random variable. The uncertainty associated with the evolution of crack length with loading cycles is taken into account by the deterioration model and through it is incorporated into the limit state function. The

material properties like fracture toughness and yield stress are also subjected to uncertainty and thus, can been modeled as random parameters.

The failure probability is then described as:

$$P_f = \mathrm{P}(G_f \leq 0) \tag{3.4}$$

This information is then used by a reliability- based lifecycle management framework to develop an optimum maintenance schedule for the component.

Besides this limit state function, another limit state function could be defined that describes the repair event. A repair action following an inspection activity is only undertaken if the crack length at the time of inspection exceeds a critical value of crack size. This limit state function could be formulated as follows:

$$G_r = a(t) - a_{cr} \tag{3.5}$$

where, $a(t)$ is the crack length at the time of inspection and a_{cr} is the critical crack repair size. However, in this study this limit state function has not be considered and it is assumed that an inspection event is always followed by a repair action. The main reason for doing so is that taking into account both the limit state functions will increase the computational burden immensely. The increase observed in the computational burden has been explained explicitly in the section 3.2. Thus, only the former limit state function that holds higher importance as it corresponds to a more catastrophic failure is considered. However, the methodology is robust enough to accommodate this modification but at the expense of higher computational cost.

3.2. Lifecycle Optimization Formulation

An optimum inspection and repair strategy is usually aimed at minimizing the total expected life cycle costs of the structure while confirming that the probability of failure at any instant during the lifetime does not exceed a maximum allowable limit. Since the optimum schedule corresponds to the minimum total expected lifecycle costs, minimization of this cost can be termed as the objective function of the optimization problem. The total life-cycle costs C_{ET} for the system is the sum of the following components: the initial costs C_I , the costs of inspections C_{INSP} , the costs of repairs C_{REP} , and the costs of failures C_F . Inspections, repairs and failures are scheduled at different times during the service life of the structure. Thus, the costs associated with each of these events occurring in the future have to be changed to match their values at the time the decision is made. This can be done by using a discount function, $e^{-\lambda t}$ where λ is the discount rate. Thus, the cost of any event at time t can be expressed as:

$$C_{event} = c_{event} e^{-\lambda t} \quad , \qquad event = \{insp, rep, fail\} \tag{3.6}$$

where, c_{event} = cost factor associated with the event. In this study, the value of $\lambda = 0.05$.

The value the objective function takes depends on both the parameters that define the inspection plan and the repair actions that are adopted following those inspection activities. The parameters defining the inspection plan are known as the design variables. An ideal way of defining the inspection schedule is deciding the time of inspections: the time to first inspection, the time to second inspection and so on and so forth. However, since similar repair and inspection tools are adopted each time the time between

consecutive inspections is usually kept the same. In this research, the inspection plan is characterized by the time to first inspection t_1 and the time between consecutive inspections δt and hence these two variables herein are the design variables of the optimization problem.

As mentioned, the value of the objective function also depends on the outcome of the inspection activities and the associated repair effort. In general, following an inspection activity, there is a likelihood that damage may or may not be detected in the structure. Depending on the damaged state of the system at the time of inspection, a decision shall be taken either to repair the system or not repair the system. The type of repair action adopted could also vary according to the damage observed in the system and so would the costs that associate with them. For instance, the repair costs would be higher if the component has failed or on the contrary it could be that if failure occurs the system is not repaired at all. Thus, in order to make credible decisions these several scenarios should be taken into account by means of a decision tree. A typical decision tree could look like Figure 3. This tree takes into account three possibilities following every inspection event: no repair, repair and replacement of component if failure occurs.

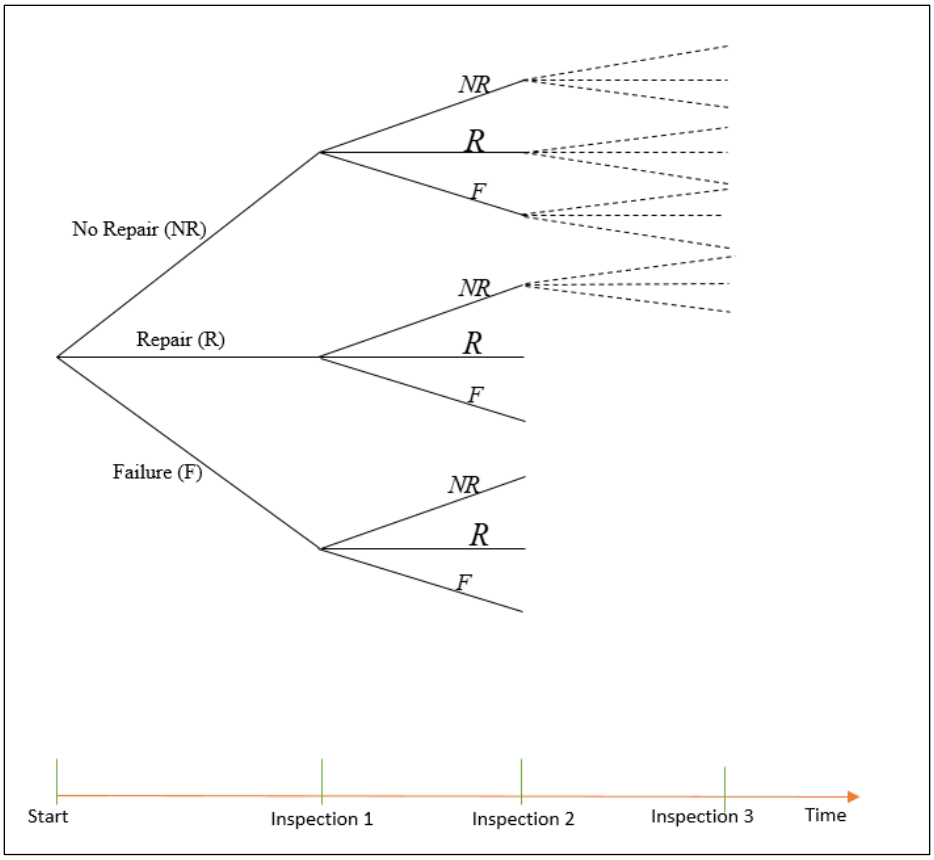

Figure 3: A Typical Decision Tree

In this research, it has been assumed that following an inspection activity a repair always take place however, the repair action is different if the component has failed. These two repair actions can also be better understood as condition-based actions and routine actions. The repair action when a component fails is undertaken when the limit-state function is violated and hence is more of a condition-based action. This action is equivalent to replacing the component. The likelihood of its occurrence is dependent on the probability of failure of the component at that instant of time. Throughout this document, the cost associated with this repair effort will be referred to as the cost of failures. The alternate repair action is always undertaken after an inspection activity and thus, is more like a

routine action and the cost associated to it will be simply referred to as the cost of repairs. A decision tree depicting these scenarios is shown in Figure 4. As it can be seen, these trees grow exponentially with the number of inspections. When only two repair efforts are considered, then the number of branches for a total of 3 inspections is 8. However, as mentioned previously if the limit state function describing the repair event was also considered separately, then there would be three scenarios to account for. These scenarios would be repair, no repair and repair effort corresponding to failure event. This means that now for 3 inspections there will be a total of 27 branches to account for. This may seem like a small increase when the number of inspections are less, however this increase is tremendous when the number of inspections increase. Thus, in this study the additional limit state function has been ignored. However, this should not be considered as a limitation as the more important limit state function has been accounted for.

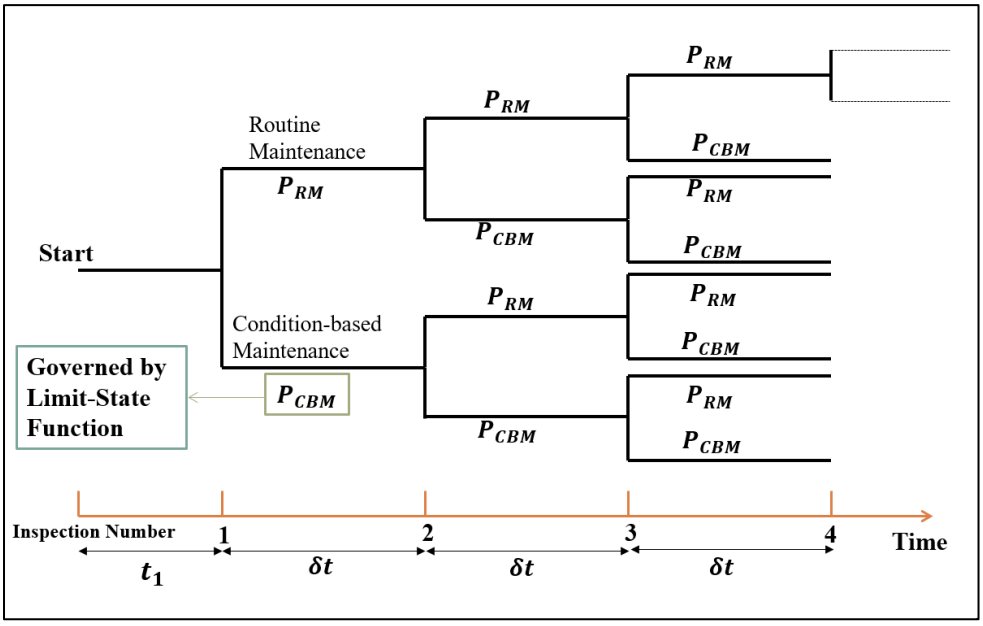

Figure 4: Diagrammatic Representation of the Scenarios considered following an inspection event in this study.

The total lifecycle costs should be evaluated taking into account all these possible scenarios and since there is a likelihood associated with the occurrence of each of these events at every instant of time, the total lifecycle costs can be better understood in an expected sense. The expected lifecycle cost can thus be defined as follows:

$$E\left[C_{ET}\right] = C_I + E[C_{INSP}] + E\left[C_{REP}\right] + E\left[C_F\right] \tag{3.7}$$

Where, $E\left[.\right]$ denotes the expectation operator.

The optimum maintenance strategy should also ensure that the maximum probability of failure throughout the lifetime never exceeds a threshold value. This can be incorporated as a constraint on the optimization problem. The optimization problem can then be formulated as follows:

$$\min_{\{t_1, \delta t\}} E\left[C_{ET}\right] \tag{3.8}$$

$$subject\ to \quad P_f \le P_{f,threshold}$$

$$t_1^{\min} \le t_1 \le t_1^{\max}$$

$$\delta t^{\min} \le \delta t \le \delta t^{\max}$$

Where, P_f is the maximum probability of failure associated with an inspection strategy, $P_{f,threshold}$ is the threshold or the target value of the maximum probability of failure, $t_1^{\min}$ and $t_1^{\max}$ are the lower and upper bounds on t_1 and similarly, $\delta t^{\min}$ and $\delta t^{\max}$ are the lower and upper bounds on δt.

3.2.1. Evaluation of Total Expected Lifecycle costs

Given the parameters of the inspection schedule $\{t_1, \delta t\}$, the value of the objective function needs to be determined. The total number of inspections scheduled over the complete design life t_d of the structure can be determined once t_1 and δt are known. Thus, the expected cost associated with the inspection events in a particular inspection plan is a deterministic value. The number of inspections can be given by:

$$N_{INSP} = 1 + floor\left(\frac{t_d - t_1}{\delta t}\right) \tag{3.9}$$

The cost of inspection can then be evaluated as:

$$E[C_{INSP}] = \sum_{i=1}^{N_{INSP}} (C_{INSP})_i \tag{3.10}$$

The evaluation of expected costs of repairs $E[C_{REP}]$ and expected cost of failures $E[C_F]$ depends on the probabilities of occurrence of the respective events at the time of inspections and also on the probability of the branch of the decision tree to which they correspond. The probability of repair at any instant can be defined as the probability of not observing any failure at that instant.

$$P_{RM} = P_{rep} = 1 - P_f \tag{3.11}$$

The cost associated with each of the event can be given by:

$$\begin{aligned} C_{REP} &= C_{rep}.P_{rep} \\ C_F &= C_{fail}.P_f \end{aligned} \tag{3.12}$$

A sample inspection plan with 3 inspections (Figure 5) has been used to illustrate the methodology used for calculating the expected costs. The methodology used has been

based on the work of Frangopol et. al [28]. At inspection 1, there are only two possible events, repair or failure represented by events e_1^1 and e_1^2 respectively. The notation used for numbering of events can be generalized as e_j^i , where j stands for the inspection number (in this case j can take values $1 to 3$) while i is used to number the events possible at the j^{th} inspection event. The value of i ranges from 1 to 2^j at the j^{th} inspection event.

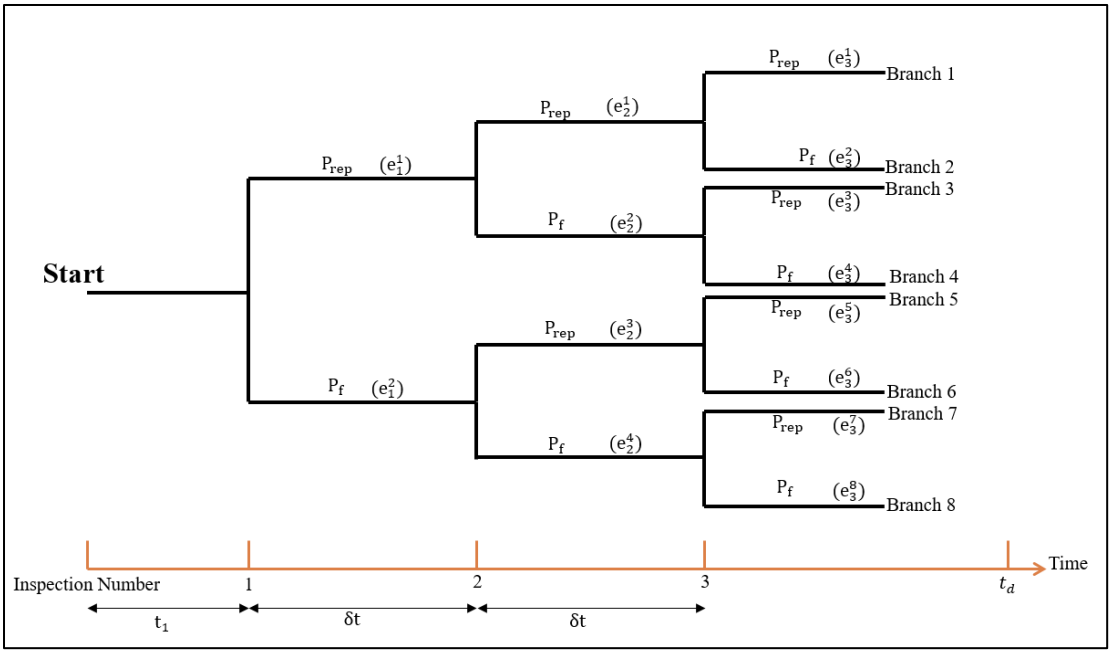

Figure 5: Event Tree for an inspection plan involving 3 inspections [28]

At inspection 2, there are 4 possible events: repair and failure events corresponding to the repair event at the last inspection, and repair and failure events corresponding to the failure event at the last inspection. These branches are denoted by $e_2^1, e_2^2, e_2^3, e_2^4$ respectively. Similarly, at the end of third inspection there are 8 possible events. The costs associated with each of these events can be found out by Eq. (3.12). It is important to note that the event tree grows exponentially, having a total of 2^j branches for an inspection strategy

involving a total of j inspections. Each of these branches is a combination of events and the probabilities of these branches can be given by:

$$\begin{aligned} &P(Branch1) = P(e_1^1).P(e_2^1).P(e_3^1) \\ &P(Branch2) = P(e_1^1).P(e_2^1).P(e_3^2) \\ &. \\ &. \\ &P(Branch8) = P(e_1^2).P(e_2^4).P(e_3^8) \end{aligned} \tag{3.13}$$

The costs associated with each of these branches can be found out by adding the cost of the events making up each branch. This cost can be given by:

$$\begin{aligned} &C(Branch1) = C(e_1^1) + C(e_2^1) + C(e_3^1) \\ &C(Branch2) = C(e_1^1) + C(e_2^1) + C(e_3^2) \\ &. \\ &. \\ &C(Branch8) = C(e_1^2) + C(e_2^4) + C(e_3^8) \end{aligned} \tag{3.14}$$

The total expected cost for the event tree can be given by:

$$E[C] = \sum_{i=1}^{8} C(Branch,i).P(Branch,i) \tag{3.15}$$

The total expected cost for any inspection strategy in general can be then given by:

$$E[C_{ET}] = C_I + \sum_{i=1}^{N_{INSP}} (C_{INSP})_i + \sum_{i=1}^{2^{N_{INSP}}} C(Branch,i).P(Branch,i) \tag{3.16}$$

The failure probabilities at the end of design life can also be determined. The maximum probability of failure associated with an inspection strategy is the maximum of the value of the failure probabilities observed over the event tree and the failure probabilities observed at the end of design life. The optimal solution should be such that this maximum probability of failure never exceeds a threshold limit.

3.3. Surrogate Model for Stochastic Optimization

The optimization problem requires several simulations to be carried out before it can accurately predict regions having low probabilities of failure. These simulations are generally very costly to run, thus making it imperative to adopt surrogate- based optimization techniques. These surrogate or meta-models can be constructed over a smaller number of simulations and thereby serve as a fast and computationally efficient alternative. Herein, the observation dataset in terms of $t_1, \delta t$, $E[C_{ET}]$ and P_f available from the simulation is used to build Gaussian process regression models. These models serve as the substitute in the optimization problem. The observation dataset can also be called as the training data set.

In general, a training dataset $\{x_i, y_i\}_{i=1}^{N}$ consists of a set of predictor or input variables x_i and response or output variables y_i. In this study, the predictor variables are $\{t_1, \delta t\}$ in each case and the response variable would be $E[C_{ET}]$ for the objective function and P_f for the constraint function. Each y_i can be represented as:

$$y_i = f(x_i) + \varepsilon \tag{3.17}$$

Where ε is the random noise component and $f(x_i)$ is known as the signal term. In linear regression model, $f(x_i)$ takes the form $a + b.x_i$, with a being representative of the intercept and b of the slope.

In a Gaussian process regression model, it is assumed $f(x_i)$ is from a Gaussian process (GP). In a Gaussian process, a distribution is defined over these functions which is updated

to get a posterior distribution when observations are available. A GP assumes that the joint probability distribution of these functions $p(f(x_1)f(x_2)....f(x_N))$ is also Gaussian with mean μ and covariance K. The mean of a Gaussian process is generally assumed to be zero unless some prior information about the process is available. There are several choices available for the covariance function of a Gaussian process. Thus,

$$f(x) \quad (3.18)$$

The basic principle underlying a Gaussian process is that if the input variables x_i and x_j are alike then the corresponding output variables will also be alike, with the similarity rooted in the covariance function [29]. Once the covariance function has been chosen, predictions can be made. For a given observation point x, the function f is known. When the predictions have to be made at a test point x^* then a new function f^* has to be defined. Using the GP framework, it can be concluded that f and f^* also follow a joint Gaussian distribution [30].

$$\begin{pmatrix} f \\ f^* \end{pmatrix} \quad \begin{pmatrix} K & K^* \\ K^{*T} & K^{**} \end{pmatrix} \quad (3.19)$$

Where, K is the matrix obtained by applying the covariance function to observed data, K^* is the matrix obtained from the covariance between the observed points and the test points and K^{**} is obtained from the covariance between the test points. The joint distributions on observed y and test y^* taking into account the noise component can be given by:

$$\begin{pmatrix} y \\ y^* \end{pmatrix} \sim \left(\begin{pmatrix} K + \sigma^2 I & K^* \\ K^{*T} & K^{**} + \sigma^2 \end{pmatrix} \right) \tag{3.20}$$

Using the standard formulation in [30], the following formulation can be obtained:

$$y^* \mid y \sim \qquad) \tag{3.21}$$

Where $\mu^* = K^{*T}(K + \sigma^2 I)^{-1} y$

$$\nu^* = K^{**} + \sigma^2 - K^{*T}(K + \sigma^2 I)^{-1} K^*$$

Many freely available software exist that can be used to train a Gaussian process regression model. Herein, the inbuilt regression toolbox of MATLAB is used to train the Gaussian process regression model. Once the surrogate model for the objective and constraint function has been constructed, it can be used by a gradient based optimization solver to solve the optimization problem given by Eq. (3.8).

4. IMPLEMENTATION AND RESULTS

4.1. Experimental Database

The experimental observations used to construct the PC expansions are obtained from the tests conducted by Virkler et.al [31] on Al 2024-T3 alloy. This dataset is an ideal choice considering its richness and its wide applicability observed in previous studies [32] [33] [34] [20] [35] to construct stochastic models representing fatigue crack growth process. The observations from the tests consisted of half crack length 'a' versus number of cycles 'N' records required to reach the particular crack length under constant amplitude loading. These observations have been plotted in Figure 7. The experimental tests were conducted on 68 similar rectangular panels having a center crack. The dimensions of the sample specimen were 558.8mm X 152.4mm X 2.54mm. The geometry of the experimental specimen is shown in Figure 6. The observations were recorded at specific crack lengths starting at an initial value of 9mm and stopping at a final value of 49.8mm. A total of 164 discrete observations existed for each specimen. Observations were recorded at an increment of 0.2mm till 36.2mm crack length, at 0.4mm increment from 36.2mm to 44.2mm and at an increment of 0.8mm for the remaining part of the experiment. The loading conditions of the experiment are summarized in table 1. The alternating load was applied at a frequency of 20 Hz. The records obtained could also be interpreted in the form of CGR versus the SIF range. The CGR $\frac{da}{dN}$ can be evaluated by finding the slope of the crack growth curve at specific points.

Table 1: Experimental Conditions [31]

Maximum load P_{max}	5.25 kips
$\Delta P = P_{max} - P_{min}$	4.20 kips
Stress Ratio $R = \frac{P_{min}}{P_{max}}$	0.2

It has been known that $\frac{da}{dN}$ as a variable is of higher interest while modeling the crack growth process than the crack length. This is because $\frac{da}{dN}$ at any value of ΔK is independent of the geometry under consideration [36]. Additionally, $\frac{da}{dN}$ against ΔK also shows a linear behavior on the log-log scale, thus the logarithm of CGR against logarithm of SIF is used as the experimental observation dataset to construct the stochastic model in this study.

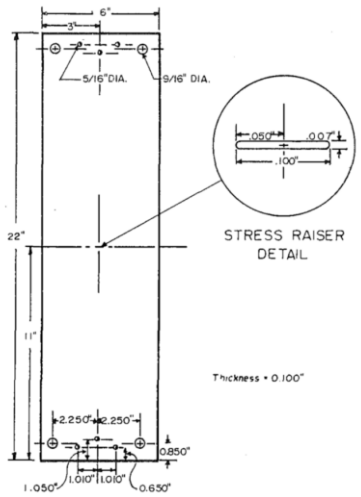

Figure 6: Details of the Experimental Specimen [31]

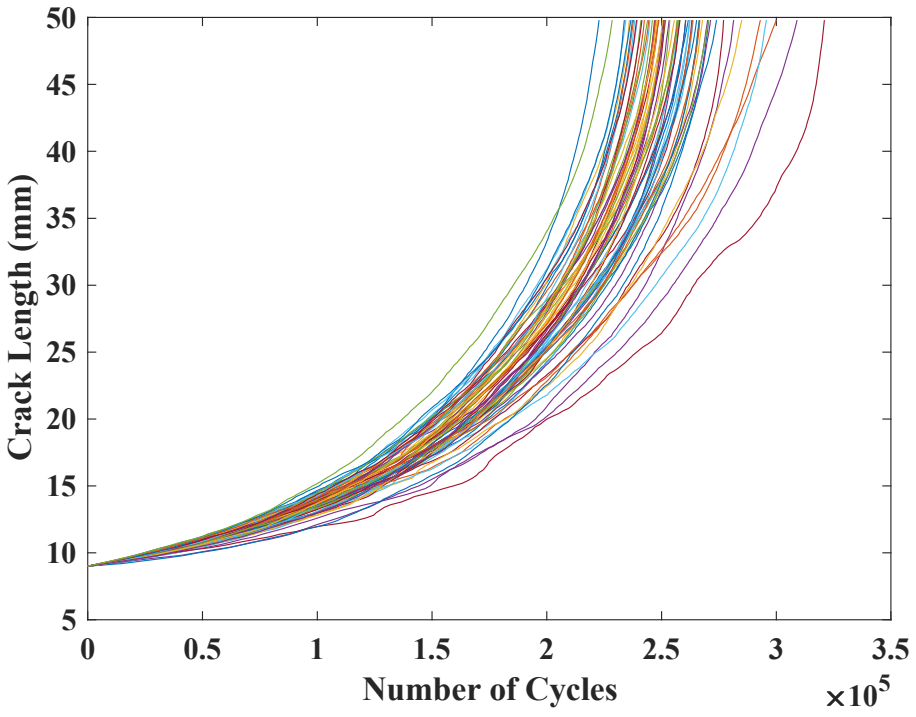

Figure 7: Experimental Crack Length versus Number of Cycle Records [31]

Several methods and their accuracy in determining CGR have been reported in literature [31]. These methods include finite difference methods and incremental polynomial methods. The predicted CGR from the model is integrated back to get the crack length and thus, the method used for calculation of the experimental CGR should be carefully selected. This method of calculation will determine the error that is inputted into the data. Incremental polynomial methods introduce higher errors as compared to finite difference methods and thus, in this research the secant method [31] is used for calculating the CGR. The average crack length $\overline{a_i}$ and the average number of cycle $\overline{N_i}$ at any point i can be determined as follows:

$$\overline{a_i} = \frac{a_i + a_{i+1}}{2}$$
$$\overline{N_i} = \frac{N_i + N_{i+1}}{2} \qquad i = 1.....163 \tag{4.1}$$

The CGR at $\overline{a_i}$ and $\overline{N_i}$ can be determined as follows:

$$\left(\frac{da}{dN}\right)_i = \frac{a_{i+1} - a_i}{N_{i+1} - N_i} \tag{4.2}$$

The data can thus be represented in the form of $\frac{da}{dN}$ versus ΔK. ΔK can be calculated at the average crack length values $\overline{a_i}$ using the following expression:

$$\Delta K = \Delta S \sqrt{\pi \overline{a_i}} . g\left(a\right) \tag{4.3}$$

Herein, ΔS is the range of the stresses applied and $g(a)$ is a correction factor that depends on the geometry of the specimen chosen.

$$\Delta S = \sigma_{\max} - \sigma_{\min} \tag{4.4}$$

$$\sigma_{\max/\min} = \frac{P_{\max/\min}}{\left(w.t\right)} \tag{4.5}$$

where, $\sigma_{\max}$ and $\sigma_{\min}$ are the maximum and minimum stresses respectively, $P_{\max}$ and $P_{\min}$ are the maximum and minimum applied loads respectively, w is the width of the plate and t is the thickness of the plate. The following geometry correction factor $g(a)$ is used to calculate ΔK in plates of finite width of $2w$ [37] (Figure 8):

$$g(a) = \left(\frac{2w}{\pi a}\right)\left(\tan\frac{\pi a}{2w}\right)^{\frac{1}{2}} \tag{4.6}$$

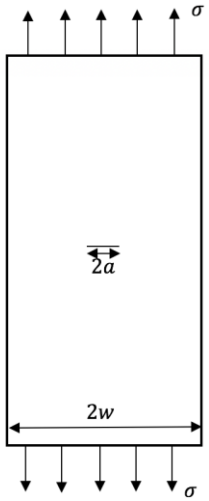

Figure 8: Finite width plate with a center crack [37]

A plot of $\ln\left(\frac{da}{dN}\right)$ against $\ln(\Delta K)$ observations that are used for constructing the stochastic model have been shown in Figure 9.

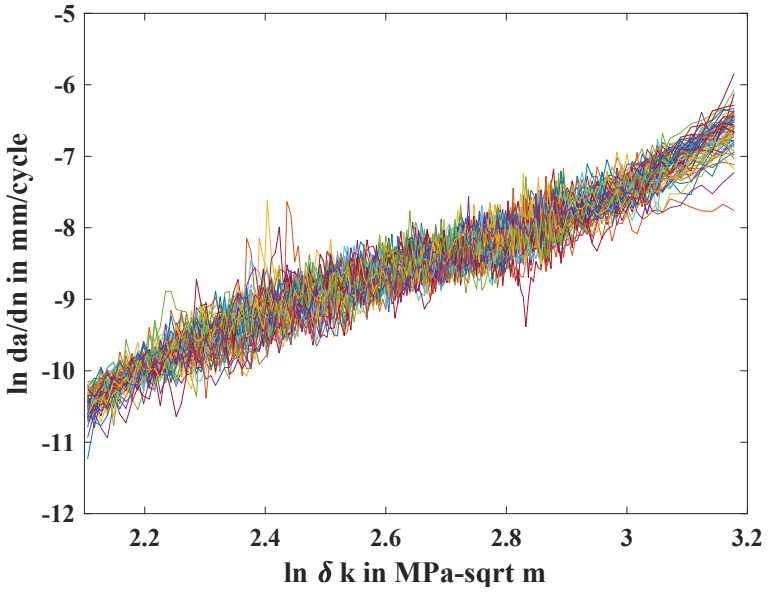

Figure 9: Log of crack growth rate versus log of stress intensity factor range from experimental data

4.2. Construction of PC representation

The ensemble of these 68 sets of $\ln\left(\frac{da}{dN}\right)$ against $\ln(\Delta K)$ observations serve as the measurement data for the random process represented by $\{Y_i\}_{i=1}^{68}$. Each of these sets represents the fatigue crack growth process discretized over a n- finite subset of the indexing variable, in this case 163 values of $\ln(\Delta K)$. Thus, each sample out of these 68 sample sets can be represented by $Y_i = [y_1^i, y_2^i .....y_n^i]^T$ where $n = 163$. Each of these components of Y_i can be represented by a PCE given by Eq. (2.14). The steps followed for the PC construction are based on [25]. In order to construct the PC expansion, firstly a scaling of sample observations is carried out to get $X_i = [x_1^i, x_2^i .....x_n^i]^T$ supported on $[-1,1]^n$. The relation between Y and X can be expressed as:

$$Y = \underline{a} + \left[(\underline{b} - \underline{a}) \circ \frac{1}{2} \right] \tag{4.7}$$

Therefore, $\{X_i\}_{i=1}^{68}$ can be obtained as:

$$X_i = 2\left[\left(Y_i - \underline{a}\right) \circ \frac{1}{(\underline{b} - \underline{a})} \right] - 1_n \;, \quad i = 1.....68 \tag{4.8}$$

The values of $\underline{a}$ and $\underline{b}$ can be given by:

$$\begin{matrix} \underline{a} = [a_1, a_2, ...a_n]^T \\ \underline{b} = [b_1, b_2, ...b_n]^T \end{matrix} \;, \quad n = 163 \tag{4.9}$$

Where, $a_i = \min(y_i^1, y_i^2, ...y_i^{68})$ and $b_i = \max(y_i^1, y_i^2, ...y_i^{68})$, $i = 1.....163$.

Following this, using the 68 observations available for each component $\{x_j\}_{j=1}^{163}$, a normalized marginal histogram is constructed for each component. The marginal PDF is obtained by linear interpolation of this histogram [38]. Once the marginal PDF is available, the PC coefficients for each of the 163 components are determined using Eq.(2.19). For the construction of PC expansion, the underlying variables are assumed to be uniform random variables and hence Legendre polynomials are the orthogonal polynomial basis chosen. Each component is then represented by the following expansion:

$$x_j = \sum_{k=0}^{P}{}^{d} c_{ki} \Psi_k(\xi_j) \tag{4.10}$$

The number of terms P retained in the expansion is a function of the order m of the polynomial and a convergence analysis is carried out to decide m. The expansions in this case have been truncated at an order $m = 8$. The results of the convergence analysis are summarized in table 2 and table 3. The mean squared errors for the mean vector and SRCC matrix calculated for different choices of PC order for the scaled observations X are plotted in Figure 10 and Figure 11. Similarly, the mean squared errors for the mean vector and SRCC matrix calculated for different choices of PC order for the sample observations Y are plotted in Figure 10 and Figure12. The marginal probability density functions of $\ln\left(\frac{da}{dN}\right)$ estimated from PC samples at selected values of $\ln(\Delta K)$ has been plotted in Figure 13.

Table 2: Relative Mean Squared Error in PC predictions of X against Experimental Data

PC ORDER	SRCC MATRIX (%)	MEAN VECTOR (%)
2	0.06057	1.7072
3	0.09609	1.2607
4	0.07616	0.4456
5	0.05829	0.3137
6	0.05511	0.2928
7	0.05506	0.2845
8	0.05509	0.2829
9	0.05506	0.2818
10	0.05510	0.2811
11	0.05509	0.2802
12	0.05508	0.2799
13	0.05506	0.2804
14	0.05506	0.2794
15	0.05506	0.2791

Table 3: Relative Mean Squared Error in PC predictions of Y against Experimental Data

PC ORDER	SRCC MATRIX (%)	MEAN VECTOR (%)
2	0.06057	2.237E-04
3	0.09609	1.353E-04
4	0.07616	5.901E-05
5	0.05829	3.581E-05
6	0.05511	3.231E-05
7	0.05506	3.185E-05
8	0.05509	3.142E-05
9	0.05506	3.142E-05
10	0.05510	3.137E-05
11	0.05509	3.118E-05
12	0.05508	3.118E-05
13	0.05506	3.115E-05
14	0.05506	3.100E-05
15	0.05506	3.096E-05

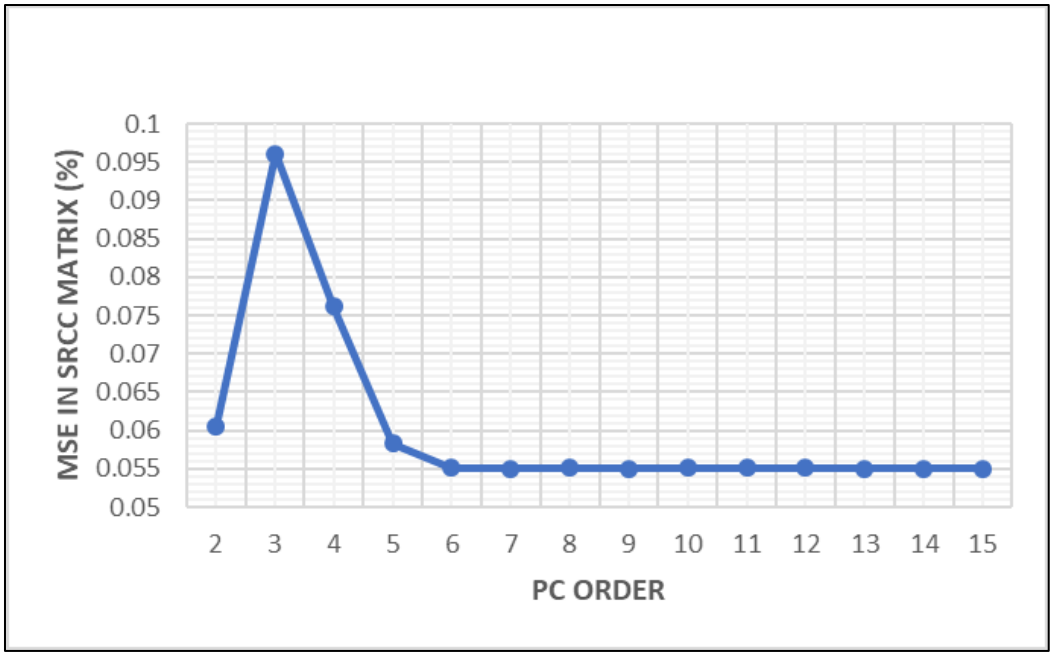

Figure 10: Graphical Plot of MSE in SRCC Matrix of X and Y against Experimental Data

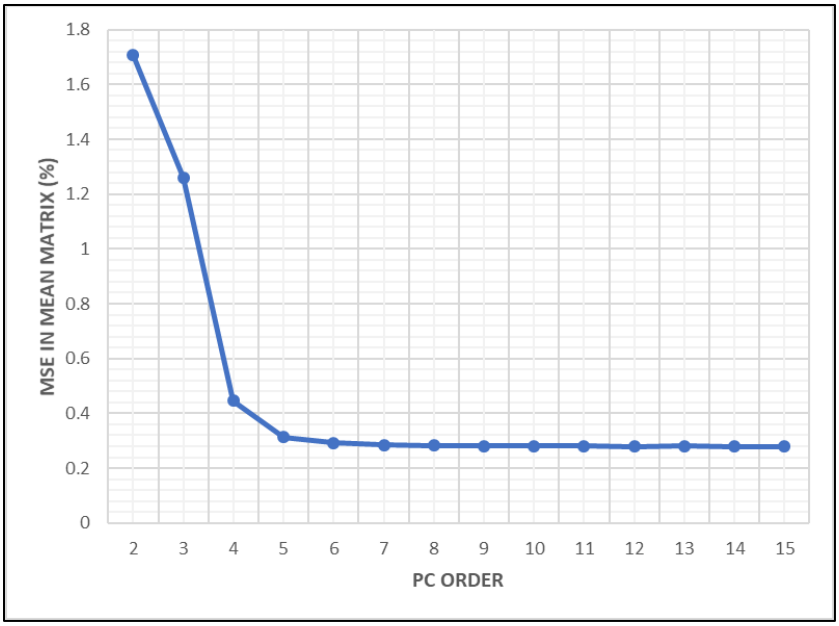

Figure 11: Graphical Plot of MSE in Mean Matrix of X against Experimental Data

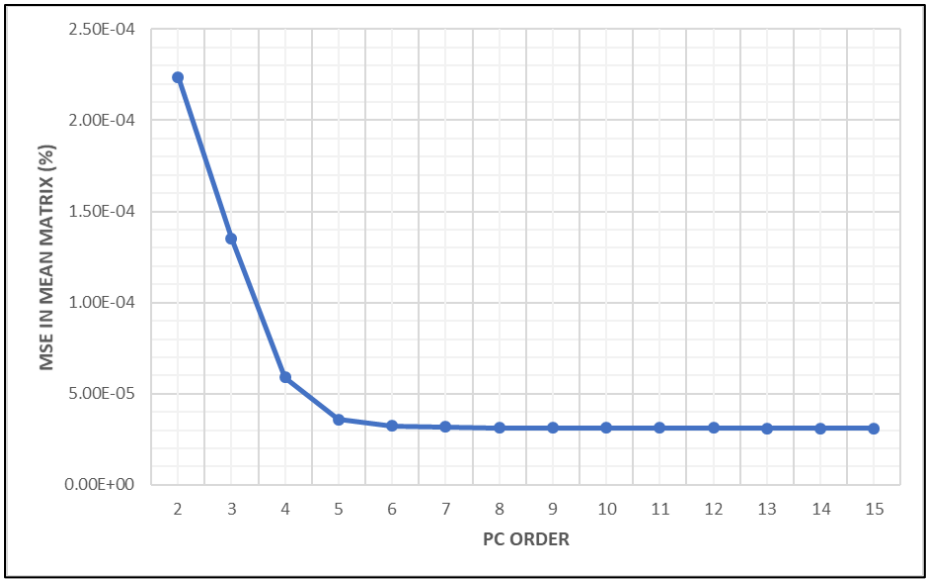

Figure 12: Graphical Plot of MSE in Mean Matrix of Y against Experimental Data

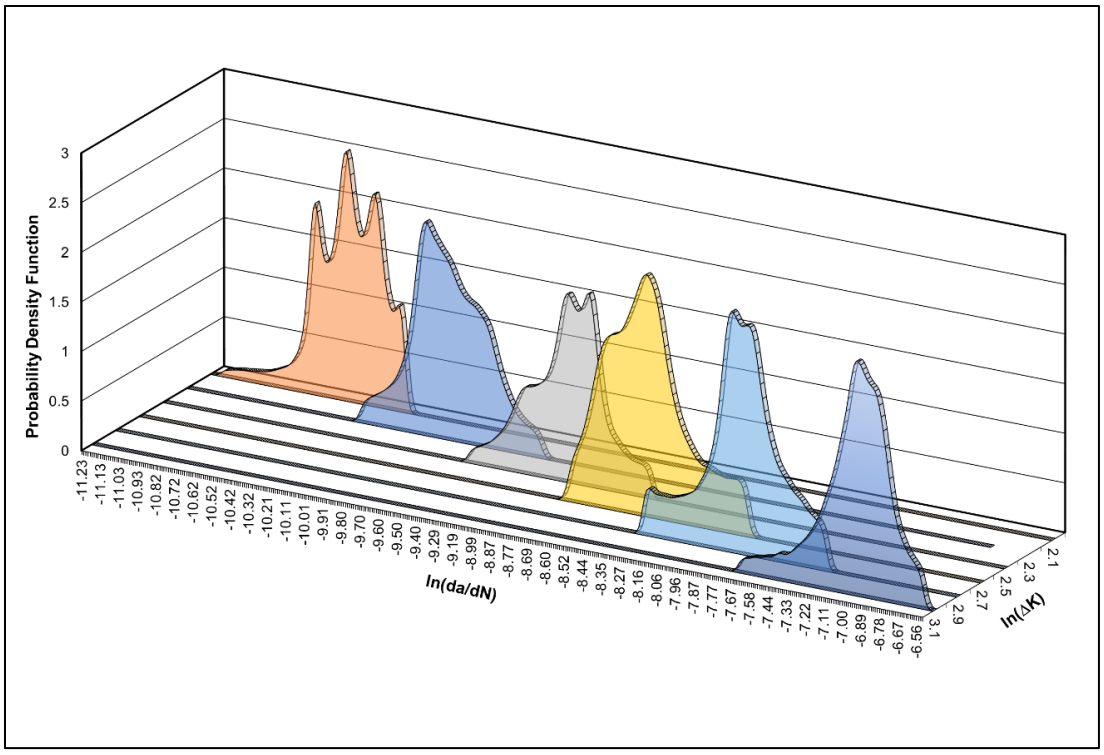

Figure 13: Evolution of marginal PDF's of logarithm of crack growth rate estimated from PC model

Once the PC expansions for each of the component has been constructed, digital realizations of X can be generated. This requires generation of correlated uniform random variables that have the same SRCC matrix as the one obtained from the experimental samples. This can be done using a normal copula technique. However, the applicability of this technique is restricted to positive-definite correlation matrices. If the SRCC matrix of X is not positive definite, then its non-positive definiteness is removed [39] and a new positive-definite correlation matrix is constructed such that the normal copula technique can be applied. This technique is known as augmented normal copula technique and has been used herein. These random variables are then incorporated into the PC expansions to generate samples of X. The digital realizations of X are then used to get the digital realizations of Y.

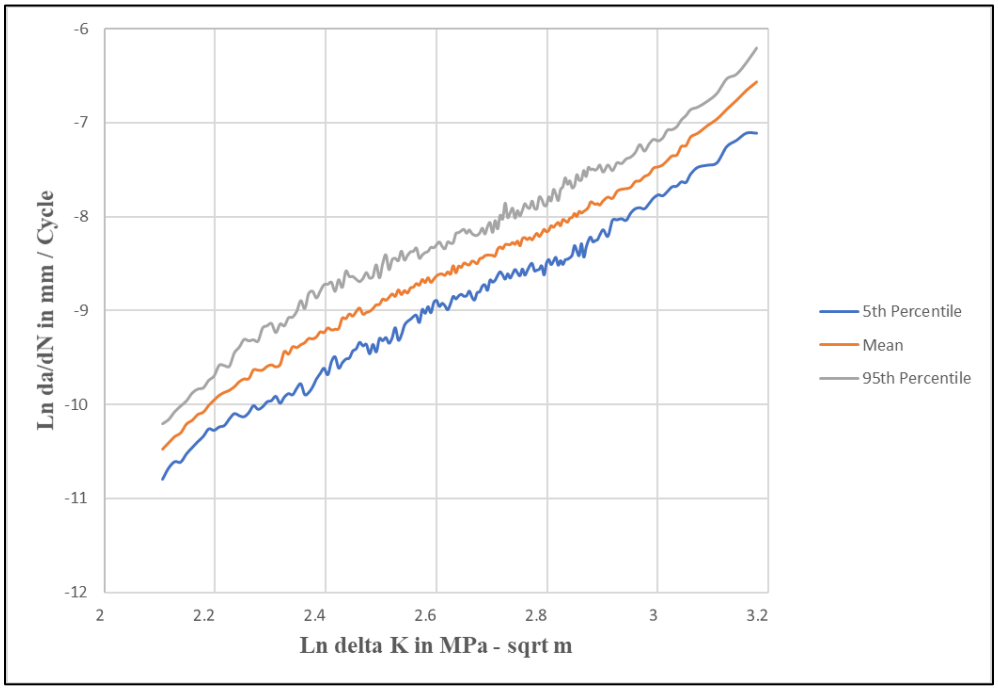

Figure 14: Confidence bounds of simulated log of crack growth rate versus log of stress intensity factor range using PC model

Figure 14 represents the predicted $\ln\left(\frac{da}{dN}\right)$ over $\ln(\Delta K)$ using the resulting PC expansion. The plot shows the mean, 5% and 95% confidence bounds. Additionally, a comparison of the two marginal PDF's obtained from the PC realizations and experimental samples is done at each value of the indexing variable and the relative MSE is computed. The minimum error observed is 0.4212% while a maximum error of 12.24% is observed. The PC coefficients are available for the n-finite subset of indexing variable $\ln(\Delta K)$ for which the experimental measurements are available. The experimental test specimens usually have larger crack or flaw sizes; thus, observations are available for larger values of ΔK. Since the initial crack sizes observed in practice are smaller, the digital realizations obtained from the PC model need to be extrapolated to model the behavior observed at smaller values of ΔK.

4.3. Application Problem

The constructed PC model can be integrated into the reliability framework to obtain the optimum maintenance and repair schedule for any system. Herein, to demonstrate the applicability of the reliability framework a simple problem is considered. The problem comprises obtaining an optimal inspection plan for an Al 2024-T3 aluminum alloy rectangular plate with a crack in the center. This has been done because the analytical geometry function for calculation of SIF for such a geometry is already known. More complex geometries could have been adopted at a higher computational cost. For such geometries, the SIF could be calculated using finite element alternating method, boundary element method or extended finite element method [9]. It is essential to note that this

geometry in spite of being very elemental is equivalent to a crack present in a pressure vessel or a crack emerging from a rivet hole [9].

The dimensions of the plate are the same as considered by Virkler et.al [31] and is given by 558.8mm X 152.4mm X 2.54mm. The initial crack length has been modeled as a random variable. The maximum design life for the component is taken as 10 years with 1.75 X 10^5 load cycles acting each year. A maximum and minimum stress of 60MPa and 12MPa respectively has been considered for loading. The random variables characterizing the problem have been summarized in Table 4.

Table 4: Random variables characterizing the application problem

Variable	Mean	Variance	Distribution	Reference
Initial Crack Length $a_0(mm)$	1.5	0.5625	Lognormal	[9]
Fracture Toughness $K_{IC}(MPa\sqrt{m})$	25	12.25	Normal	[40]
Yield Strength $\sigma_y(MPa)$	332	1102.24	Normal	[41]

4.4. Implementation of lifecycle optimization

The constructed PC model gives simulated samples of the natural logarithm of CGR with respect to natural logarithm of SIF range. In order to get the crack length versus number of cycle's records, the CGR needs to be integrated in terms of the number of cycles. Herein, the CGR is integrated over every 1000 cycles. The forward Euler method is adopted for carrying out the integration [42]. The integration could have been done over a smaller number of cycles, however that increases the computational burden immensely

and is thus avoided. Since the number of cycles is a function of time, the crack length at any time can hence be known. Thereby, the PC model is used to obtain the crack evolution in time and through this time evolution of crack, the uncertainty in the process is incorporated into the limit state function. The limit state function as described previously is a random function, and thus there is a likelihood associated with occurrence of the failure event at any time t . The probability of failure event can be found out using Monte Carlo simulations.

To this end, 100,000 trajectories of the stochastic process are generated using the PC model. Similarly, the random variables given by table 4 are also sampled. Using the information available on the initial crack size and the trajectories of the stochastic process, the trajectories of crack evolution in time are obtained. For any given value of $\{t_1, \delta t\}$, the timing of inspection events is known. At the time of inspection, the probability of failure can be approximated numerically as the ratio of number of failed samples to the total number of samples. After an inspection event, the component is brought back to its original state, which is the crack length is reset by resampling and new crack growth trajectories are generated from that time onwards. However, if the component fails then not only the crack growth histories are regenerated but the material properties are also resampled. As mentioned previously, the decision at the time of next inspection event will be dependent on the past inspection event and all these scenarios can be taken into account through an event tree. The total expected lifecycle cost associated with a specific value of $\{t_1, \delta t\}$ can be determined through the methodology described in Section 3.2.1. The initial

cost of the system is taken as 1. The cost factors associated with different events used for the evaluation of the total expected lifecycle costs are summarized in Table 5.

Table 5: Multiplicative cost factors used for calculation of total expected lifecycle cost [1]

Event	Cost factor	Value
Inspection	c_{insp}	0.025
Repair	c_{rep}	0.25
Failure	c_f	50

To obtain the optimal maintenance schedule, the total expected lifecycle costs need to be evaluated at different values of $\{t_1, \delta t\}$ and compared. Thus, an exhaustive search is carried out. This exhaustive search enables in studying the complete design space. The values of total expected life-cycle cost are evaluated over a grid of design variables $\{t_1, \delta t\}$, where $t_1 \in \{1/12, 4.5\}$ years and $\delta t \in \{0.5, 5.25\}$ years. An increment of 0.25 years is taken for each variable, giving a complete grid of 18 X 20 points. For this grid, the response surface associated with the objective function was constructed. This plot is shown in Figure 15.

Using this plot, the minimum expected cost could be identified that would satisfy the constraint function as well. In this study, the threshold on maximum probability of failure has been considered as 0.05 or 5%. Thus, the optimal schedule will not only confirm that the maximum probability of failure during the lifetime never exceeds this value but will also correspond to the least total expected lifecycle cost.

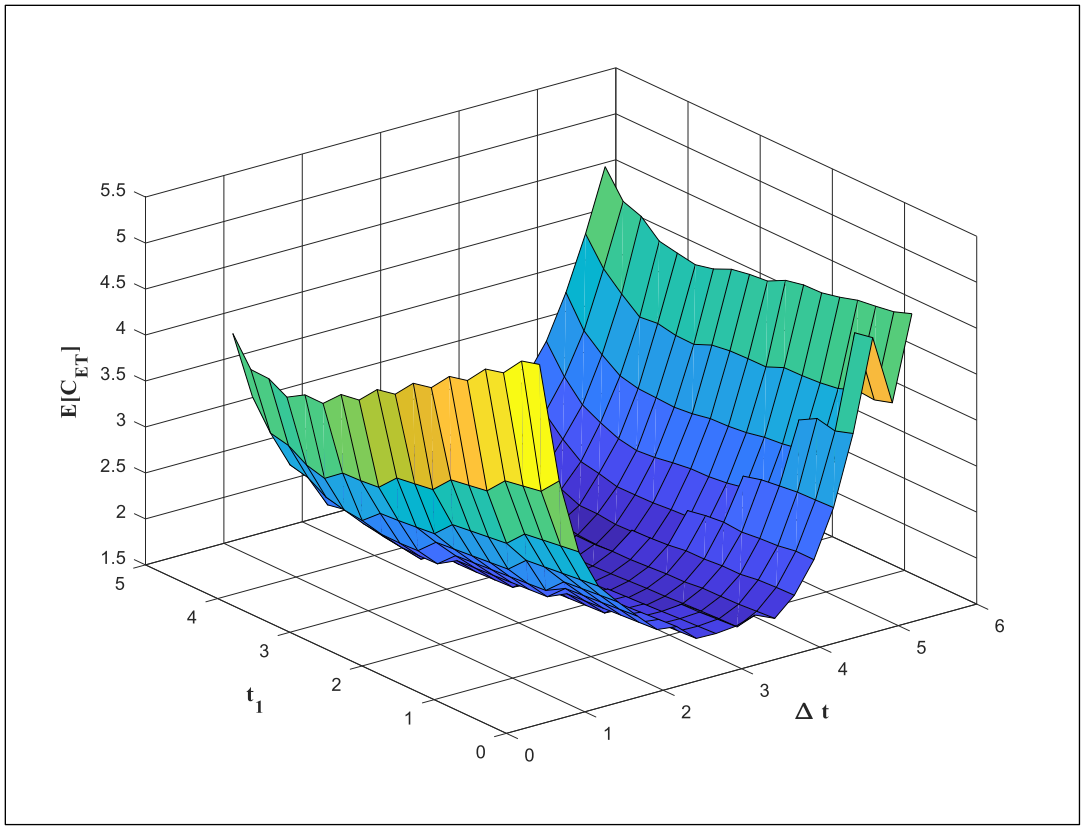

Figure 15: Response Surface for objective function (total expected cost)

The minimum total expected cost is found as $E[C_{ET}] = 1.6387$ at $\{t_1, \delta t\} = \{2.83, 2.75\}$ years. The corresponding value of $P_{f,\max}$ is 0.0179. In order to better visualize the variation of total expected lifecycle cost with δt at a given value of t_1, the slice of the surface corresponding to $t_1 = 2.83$ years has been plotted in Figure 16.

However, exhaustive search is not an ideal way of finding the optimal solution. This method has a high computational cost and is not feasible if the resolution of the grid has to be increased. The construction of response surface for the above mentioned grid takes about 30 hours using computing resources provided by Texas A&M High Performance

Research Computing. Thus, a surrogate model is adopted to perform the gradient based optimization.

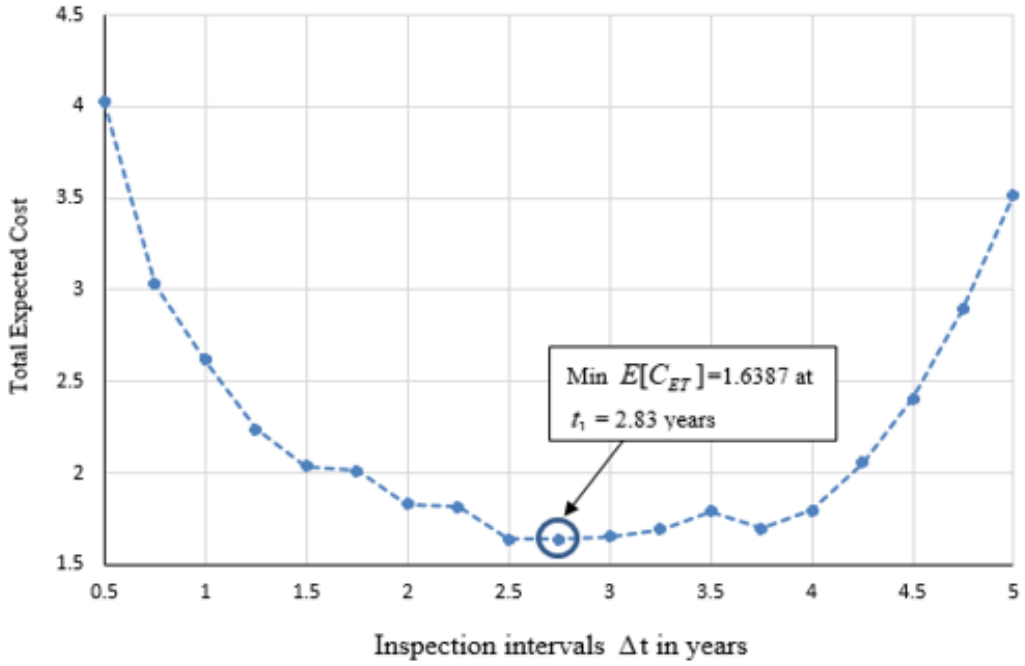

Figure 16: The variation of total expected cost with inspection intervals at optimum value of t_1

4.5. Optimization under uncertainty via surrogate model

A Gaussian process regression model is used to construct the surrogate models for the objective and the constraint function based on the methodology described in Section 3.3. The predictive capability of the Gaussian process depends exclusively on the suitability of the chosen kernel or covariance function. In this study, the matern 5/2 kernel function has been chosen. A root mean squared error of 0.12 is reported for the Gaussian surrogate model constructed for the total expected cost surface. Figure 17 can be used to verify the performance of the model constructed for total expected cost surface. The predicted

response is shown by the diagonal line, while the vertical distance of the observations from the line is a measure of the error in prediction at that point.

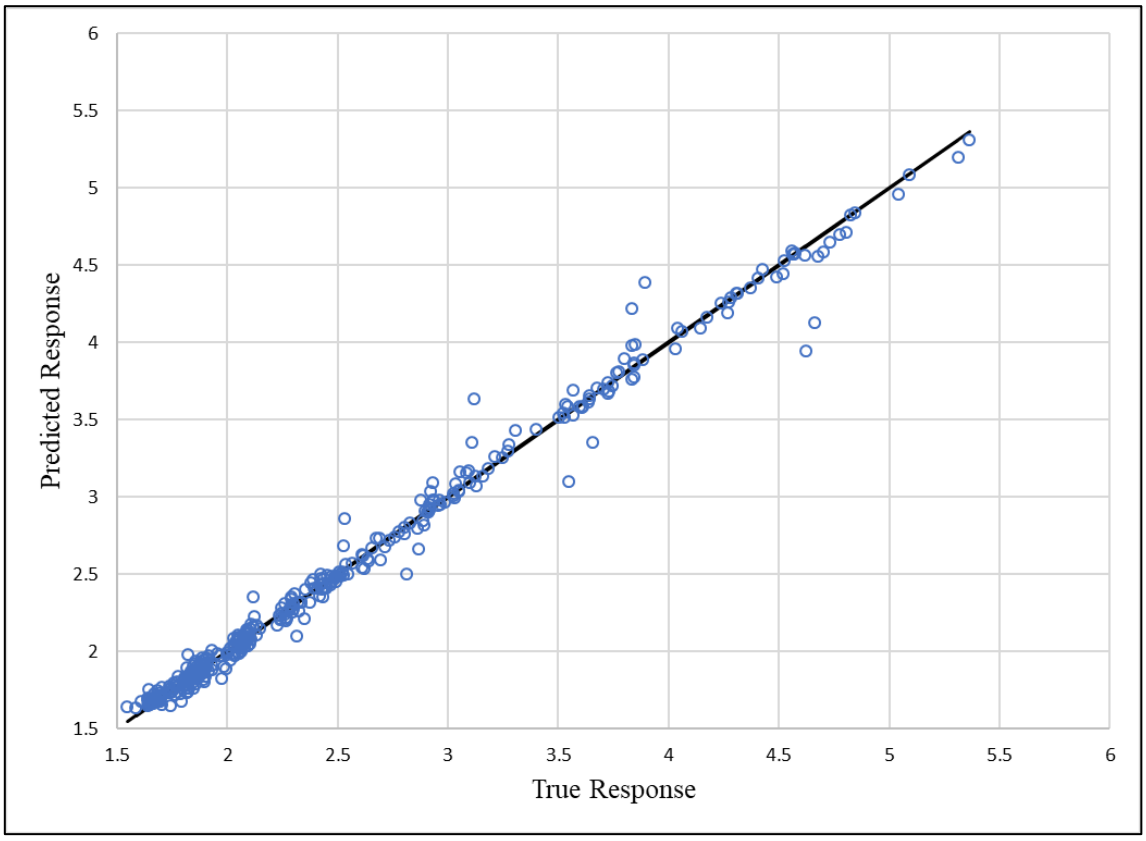

Figure 17: Predicted versus Actual Plot (Total Expected Lifecycle Cost)

The reconstructed surface for the total expected cost has been shown in Figure 18. Similarly, the reconstructed surface for the maximum probability of failure is shown by Figure 19.

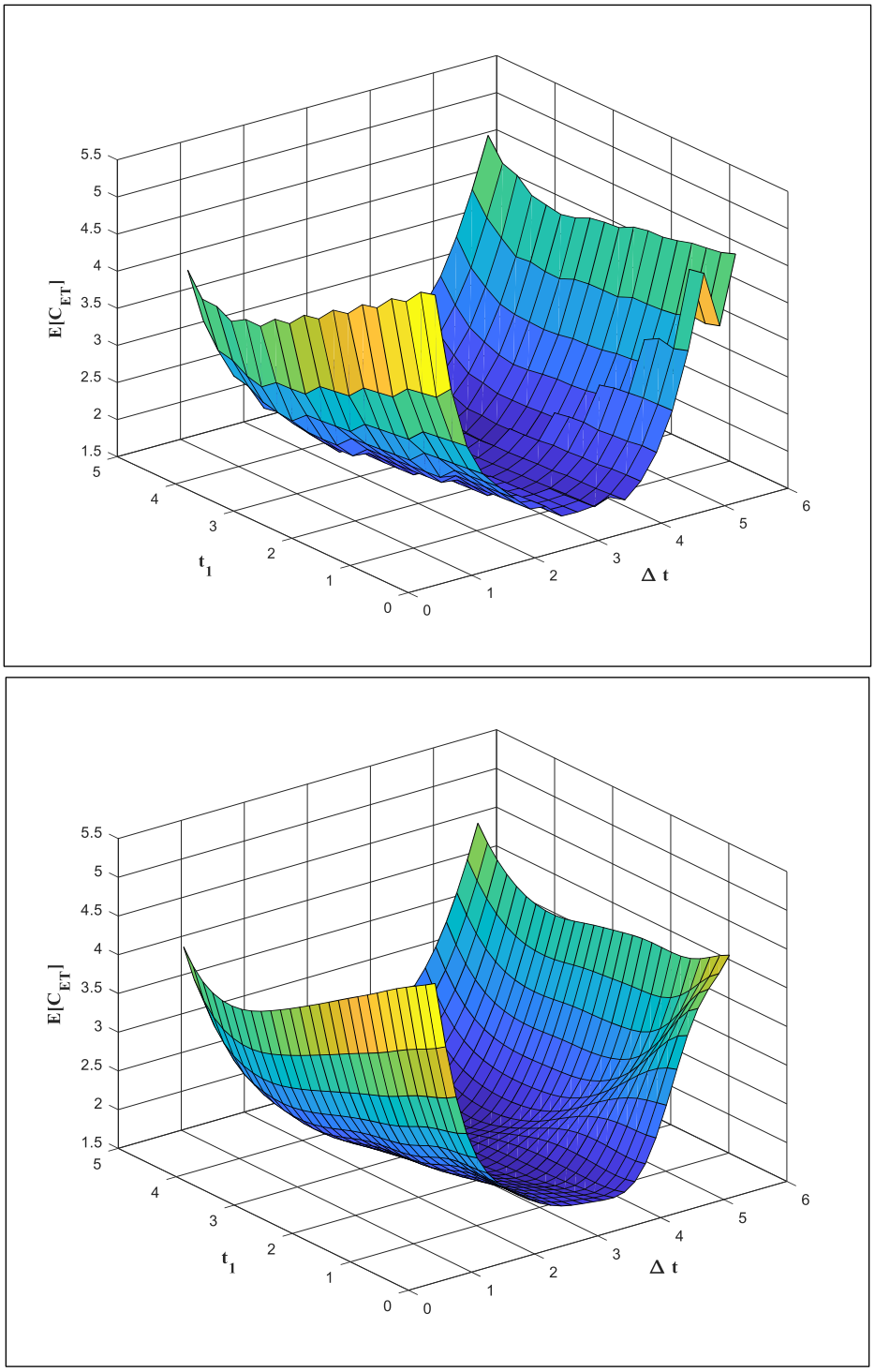

Figure 18: Response Surface of Total Expected Cost (Objective Function): Exact (top) and reconstructed with Gaussian process regression model (bottom)

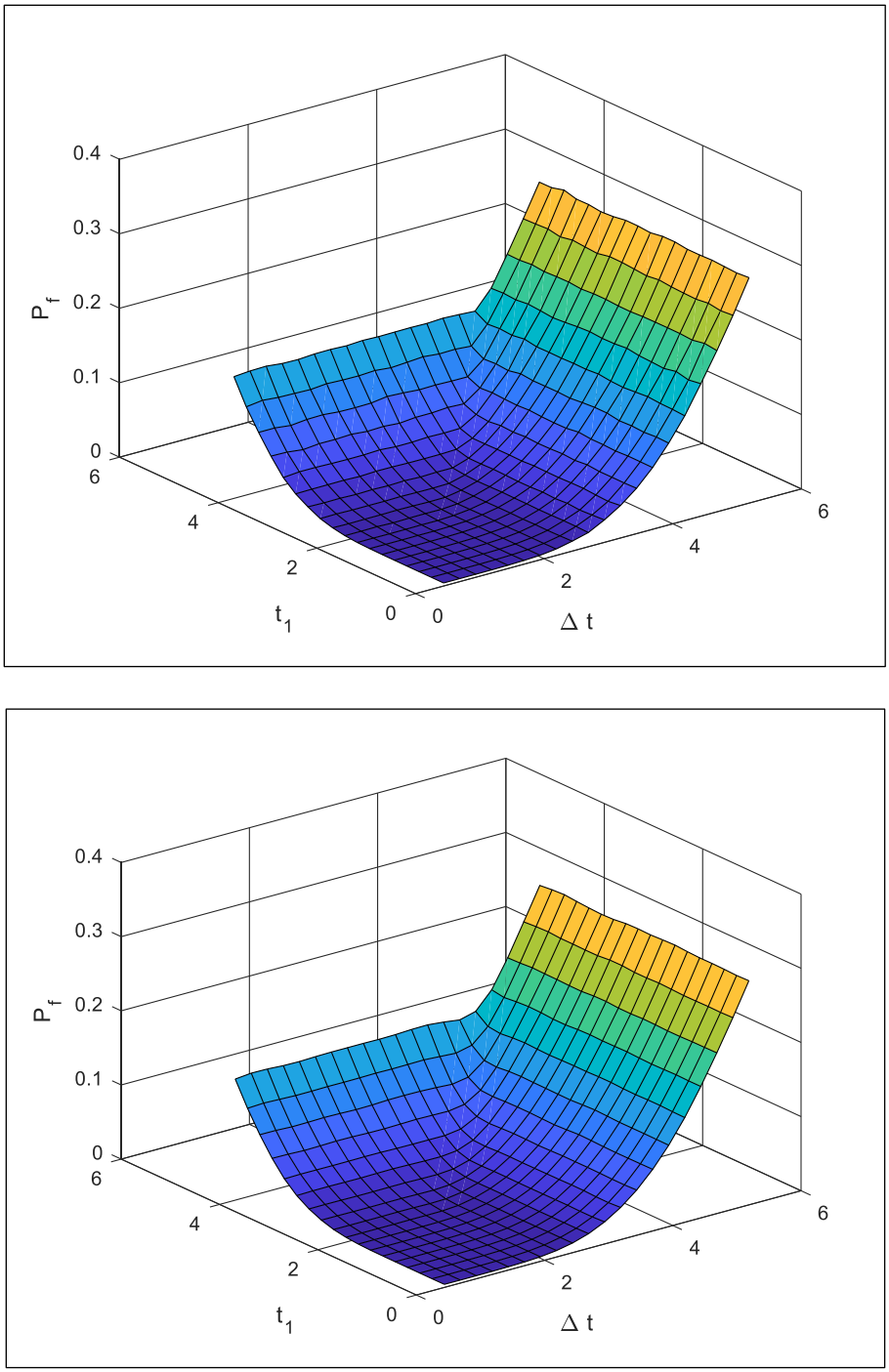

Figure 19: Response Surface of Probability of failure (Constraint Function): Exact (top) and reconstructed with Gaussian process regression model (bottom)

These surrogate or meta-models are now used for solving the gradient-based optimization. The optimization has been carried out for 4 different thresholds on the maximum probability of failure. The values are $P_{f,threshold} = \{0.05, 0.01, 0.005, 0.001\}$. The accuracy of the optimum solution is dependent upon the approximation accuracy of the surrogate and the result obtained is an approximation of the true optimum. Table 6 summarizes the optimum results and corresponding minimum total expected lifecycle cost obtained for different thresholds on maximum probability of failure through exhaustive search method. Similarly, Table 7 summarizes the results obtained for the same thresholds on maximum probability of failure through gradient- based optimization. The results obtained through both the methods are comparable.

Table 6: Optimization Results for different values of thresholds on maximum probability of failure using exhaustive search method

$P_{f,threshold}$	t_1 in years	Δt in years	$E[C_{ET}]$
0.05	2.83	2.75	1.639
0.01	2.33	2.5	1.817
0.005	2.08	2.25	1.840
0.001	1.58	1.75	2.073

Table 7: Optimization Results for different values of thresholds on maximum probability of failure using gradient-based optimization

$P_{f,threshold}$	t_1 in years	Δt in years	$E[C_{ET}]$
0.05	2.80	2.79	1.649
0.01	2.45	2.53	1.708
0.005	2.20	2.28	1.819
0.001	1.60	1.77	2.096

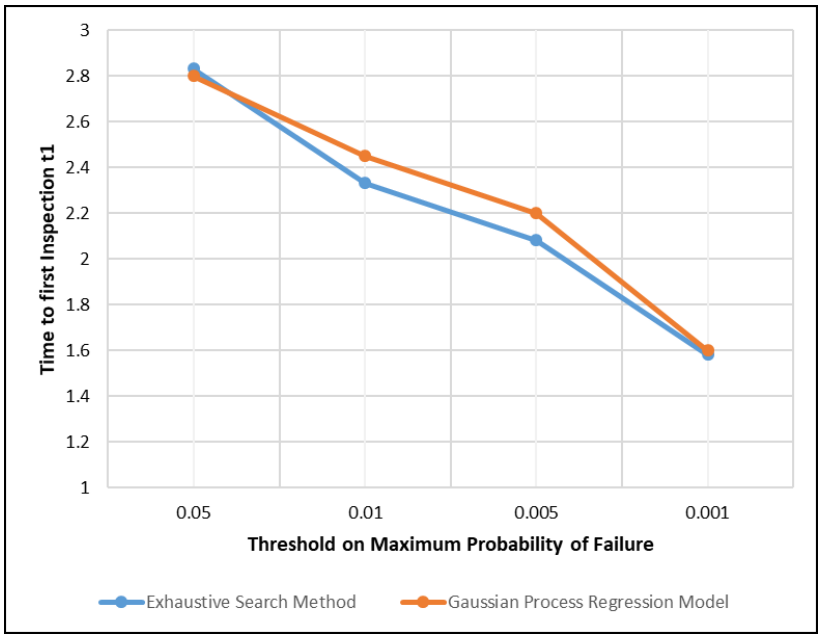

Figure 20: The sensitivity of t_1 with respect to the thresholds on maximum probability of failure

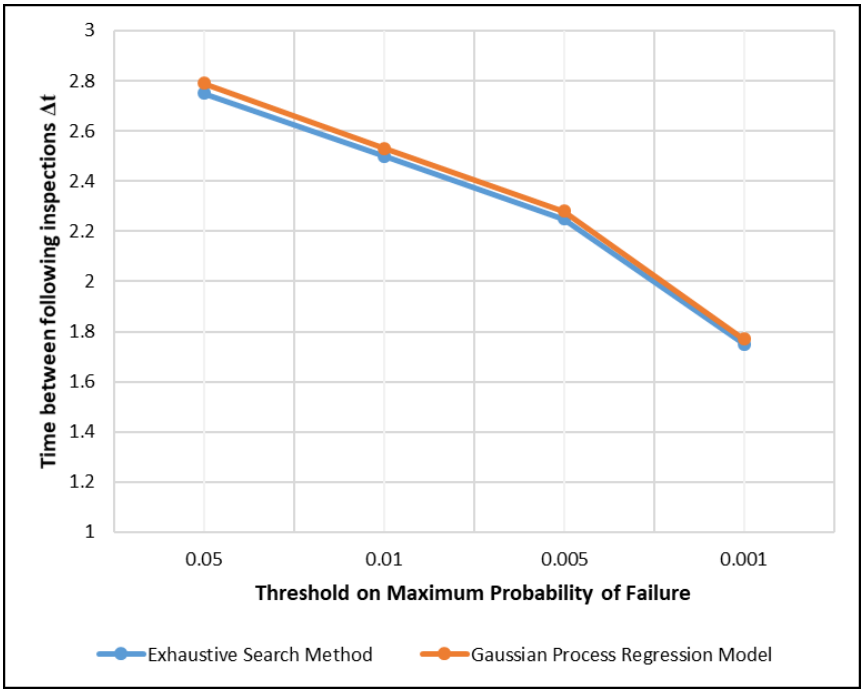

Figure 21: The sensitivity of Δt with respect to the thresholds on maximum probability of failure

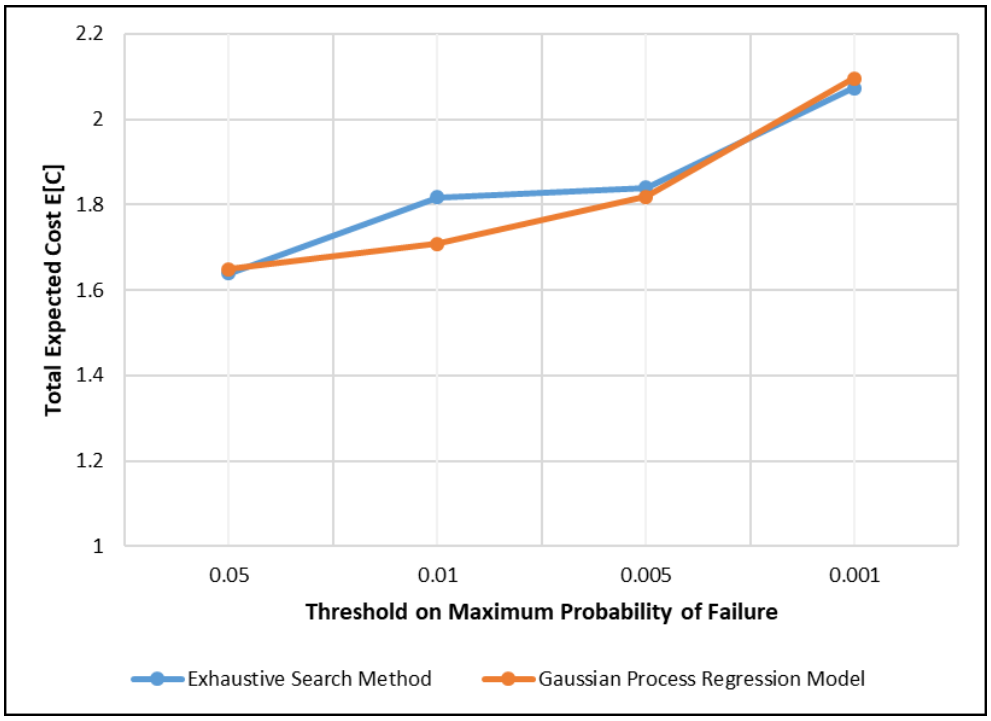

Figure 22: The sensitivity of E[C_{ET}] with respect to the thresholds on maximum probability of failure

The sensitivity of $t_1, \Delta t$ and $E[C_{ET}]$ to different thresholds on the maximum probability of failure has been plotted in figure 20, figure 21 and figure 22 respectively. It is clearly evident from the results obtained that the total expected lifecycle costs increase when the threshold is reduced. The time between the inspections also decreases correspondingly. This can be explained by the fact that the structure would now require more frequent inspection and maintenance activities to stay within the prescribed threshold on probability of failure. Thus, it can be seen that there is a compromise between a higher reliability and the minimum total expected lifecycle costs.

5. CONCLUSIONS

This research develops a framework that uses a reliability-based approach to address the lifecycle management of components subjected to fatigue-induced damage. The crack growth process is highly uncertain and the uncertainty is efficiently captured by modeling it as polynomial chaos expansions. Through the PC representations, the uncertainty is propagated into the model predictions and hence into the limit state functions. The optimum solution corresponds to minimum total expected lifecycle costs that include the costs of inspections, repairs and failures. This analysis takes into account the time value of money and different repair scenarios. The optimum results are defined in terms of time to first inspection and the time between consecutive inspections. A computationally efficient optimization strategy is proposed to solve the stochastic optimization associated with the optimal scheduling. This strategy uses Gaussian process regression models as surrogates for the objective and constraint function. This considerably reduces the computational burden of the problem. The sensitivity of the optimal solution to different thresholds on the maximum probability of failure is also examined. It is observed that the total expected lifecycle costs increase when the target value of maximum probability of failure is reduced. Thus, there is always a trade-off between higher reliability and minimum total expected lifecycle costs. The proposed framework shows immense potential of integrating economic and risk aspects of design. This framework makes no prior assumptions and its predictive capability completely relies on the quality of the input data. Most importantly, the proposed reliability-based framework can be readily modified

to address the lifecycle optimization of any system be it bridges, ships or girders. The applicability of the framework is also not limited to just deterioration due to fatigue. It can be extended to any time-dependent deterioration mechanism that causes damage-induced structural failure over lifetime like corrosion or corrosion-fatigue. The universal nature of this framework makes it a very efficient and robust tool.

6. REFERENCES

[1] M. K. &. J. N. D.M. Frangopol, "Probabilistic models for life-cycle performance of deteriorating structures :review and future directions," *Progress in Structural Engineering and Materials,* vol. 6, no. 4, pp. 197-212, 2004.

[2] D. S. &. M. H. Faber, "Computational aspects of risk-based inspection planning," *Computer-Aided Civil and Infrastructure Engineering,* vol. 21, pp. 179-192, 2006.

[3] D. S. &. M. H. Faber, "Risk based inspection planning for structural systems," *Structural Safety,* vol. 27, pp. 335-355, 2005.

[4] D. Y. Y. &. D. M. Frangopol, "Probabilistic optimization framework for inspection/repair planning of fatigue-critical details using Bayesian networks," *Computers and Structures,* vol. 198, pp. 40-50, 2018.

[5] Y. D. &. D. M. Frangopol, "Risk-informed life-cycle optimum inspection and maintenance of ship structures considering corrosion and fatigue," *Ocean Engineering,* vol. 101, pp. 161-171, 2015.

[6] R. T. &. E. C. H.O Madsen, "Probability-based cost benefit analysis of fatigue, design and inspection," in *Marine structural Inspection, Maintenance and Monitoring Symposium*, Arlington, 1991.

[7] K. L. &. A. E. D.M. Frangopol, "Reliability of reinforced concrete girders under corrosion attack," *Journal of Structural Engineering,* vol. 123, no. 3, pp. 286-297, 1997.

[8] D. D. G. &. D. S. S. Dr. E. Nikolaidis, Engineering Design Reliability Handbook, CRC Press, 2004.

[9] W. J. &. A. T. B. Gomes, "Optimal inspection planning and repair under random crack propagation," *Engineering Structures,* vol. 69, pp. 285-296, 2014.

[10] M. V. G. S. &. H. J. P. Beaurepaire, "Reliability-based optimization of maintenance scheduling of mechanical components under fatigue," *Computer Methods in Applied Mechanics and Engineering,* Vols. 221-222, pp. 24-40, 2014.

[11] M. V. &. G. Schueller, "Design of maintenance schedules for fatigue prones mettalic components using reliability based optimization," *Computer Methods in Applied Mechanics and Engineering,* vol. 199, no. 33-36, pp. 2305-2318, 2010.

[12] P. P. &. F. Erdogan, "A critical analysis of crack propagation laws," *Journal of Basic Engineering,* vol. 85, no. 4, pp. 528-533, 1963.

[13] N. a. K. R. Vikram, "Review on Fatigue Crack Growth and Finite Element Method," *International Journal of Scientific \& Engineering Research,* vol. 4, no. 4, pp. 833-843, 2013.

[14] H. G. a. S. Dore, "Probabilistic Description of fatigue crack growth in polycrystalline solids," *Engineering Fracture Mechanics,* vol. 21, no. 6, pp. 1151-1168, 1985.

[15] J. W. Provan, Probabilistic Fracture Mechanics & Reliability, Dordrecht: Springer, 1987.

[16] J. Y. &. S. Manning, "A simple second order approximation for stochastic crack growth analysis," *Engineering Fracture Mechanics,* vol. 53, no. 5, pp. 677-686, 1996.

[17] F. K. &. J. Bogdanoff, "A critical analysis of some probabilistic models of fatigue crack growth," *Engineering Fracture Mechanics ,* vol. 14, pp. 59-89, 1981.

[18] H. G. &. J. Provan, "Micromechanics theory of fatigue crack initiation and propagation," *Engineering Fracture Mechanics ,* vol. 13, no. 4, pp. 963-977, 1980.

[19] M. G. &. F. Penta, "A gamma process model for the analysis of fatigue crack growth data," *Engineering Fracture Mechanics,* vol. 142, pp. 21-49, 2015.

[20] K. O. a. A. S. Kiremidjian, "Stochastic modeling of fatigue crack growth rate," *Engineering Fracture Mechanics,* vol. 29, no. 3, pp. 317-334, 1988.

[21] K. O. &. A. Kiremidjian, "A stochastic model for fatigue crack growth rate data," *Journal of Engineering for Industry,* vol. 109, pp. 13-18, 1987.

[22] R. G. Shigehiro Sakamoto, "Polynomial chaos decomposition for the simulation of non-Gaussian nonstationary stochastic processes," *Journal of Engineering Mechanics,* vol. 128, no. 2, pp. 190-201, 2002.

[23] R. G. &. P. Spanos, "Spectral techniques for Stochastic finite elements," *Archives of Computational Methods in Engineering,* vol. 4, no. 1, pp. 63-100, 1997.

[24] O. L. M. &. O. Knio, Spectral Methods for Uncertainty Quantification: with Applications to Computational Fluid Dynamics, Springer Science & Business Media, 2010.

[25] R. G. &. S. F. Sanjoy Das, "Polynomial chaos representation of spatio-temporal random fields from experimental observations," *Journal of Computational Physics,* vol. 228, pp. 8726-8751, 2009.

[26] M. Rosenblatt, "Remarks on a multivariate transformation," *The Annals of Mathematical Statistics,* vol. 23, no. 3, pp. 470-472, 1952.

[27] T. Anderson, Fracture Mechanics: fundamentals and applications, CRC Press, 1991.

[28] K. L. &. A. E. D.M Frangopol, "Life-cycle cost design of deteriorating structures," *Journal of Structural Engineering ASCE,* vol. 123, pp. 1390-1401, 1997.

[29] K. P. Murphy, Machine Learning: A Probabilistic Perspective, Massachusetts: MIT Press, 2012.

[30] C. R. &. C. Williams, Gaussian Processes for Machine Learning, Cambridge,Massachusetts: MIT Press, 2006.

[31] B. H. &. P. G. D.A. Virkler, "The statistical nature of fatigue crack propagation," *Journal of Engineering Materials and Technology,* vol. 101, pp. 148-153, 1979.

[32] A. T. B. &. W. J. d. S. Gomes, "Stochastic fracture mechanics using polynomial chaos," *Probabilistic Engineering Mechanics,* vol. 34, pp. 26-39, 2013.

[33] Z. A. Kotulski, "On effieciency of identification of a stochastic crack propagation model based on Virkler experimental data," *Archives of Mechanics,* vol. 50, no. 5, pp. 829-847, 1998.

[34] F. P. &. G. M. Grasso, "A four-parameters model for fatigue crack growth analysis," *Frattura ed Integrità Strutturale,* vol. 26, pp. 69-79, 2013.

[35] S. T. &. s. P. Asok Ray, "Stochastic modeling of fatigue crack propagation," *Applied Mathematical Modeling,* vol. 22, pp. 197-204, 1998.

[36] B. H. &. P. G. D.A. Virkler, "The statistical Nature of fatigue crack propagation," Air Force Flight Dynamics Laboratory, West Lafayette, 1978.

[37] J. B. &. S. Rolfe, Fracture and fatigue control in structures: Applications of fracture mechanics, Philadelphia: ASTM, 1999.

[38] L. E. P. &. F. T. U. Yanni Kouskoulas, "A Computationally Efficient Multivariate Maximum-Entropy Density Estimation (MEDE) Technique," *IEEE Transactions on Geoscience and Remote Sensing,* vol. 42, no. 2, pp. 457-468, 2004.

[39] L. V. &. S. Boyd, "Semidefinite Programming," *SIAM Review,* vol. 38, no. 1, pp. 49-95, 1996.

[40] W. Schutz, "Treatment of fracture toughness data for design purpose," in *Practical Applications of Fracture Mechanics*, AGARD-AG-257 , H. Liebowitz(ed.), 1980.

[41] C. Proppe, "Probabilistic analysis of multi-site damage in aircarft fuselages," *Computational Mechanics,* vol. 30, pp. 323-329, 2003.

[42] F. A. V. N. H. K. Matthew J. Pais, "Enabling high-order integration of fatigue crack growth with surrogate modeling," *International Journal of Fatigue,* vol. 43, pp. 150-159, 2012.